DR. HYUNG-GEUN MOON (Orcid ID : 0000-0003-3752-3035)

Article type : Original Article: Asthma and Lower Airway Disease

Colony stimulating factor 1 and its receptor are new potential therapeutic targets for allergic asthma

Hyung-Geun Moon[1*], Seung-jae Kim[1], Myoung Kyu Lee[1], Homan Kang[2], Hak Soo Choi[2], Anantha Harijith[3], Jinhong Ren[4], Viswanathan Natarajan[1,5], John W. Christman[6], Steven J. Ackerman[7], Gye Young Park[1*]

[1]Division of Pulmonary, Critical Care, Sleep and Allergy, Department of Medicine, University of Illinois at Chicago, Chicago, IL, USA

[2]Gordon Center for Medical Imaging, Department of Radiology, Massachusetts General Hospital and Harvard Medical School, Boston, MA, USA.

[3]Department of Pediatrics, University of Illinois at Chicago, IL, USA

[4]Center for Biomolecular Science, College of Pharmacy, University of Illinois at Chicago, IL, USA

[5]Department of Pharmacology, University of Illinois at Chicago, IL, USA

[6]Section of Pulmonary, Critical Care, and Sleep Medicine, the Ohio State University, Davis Heart and Lung

[7]Department of Biochemistry and Molecular Genetics, and Medicine, University of Illinois at Chicago, IL, USA

Research Center, Columbus, Ohio, USA

This article has been accepted for publication and undergone full peer review but has not been through the copyediting, typesetting, pagination and proofreading process, which may lead to differences between this version and the Version of Record. Please cite this article as doi: 10.1111/all.14011
This article is protected by copyright. All rights reserved.

Accepted Article

Accepted Article

*These authors contributed equally.

Running title: Inhibition CSF1-CSF1R axis for asthma therapy

Corresponding author: Hyung-Geun Moon, Ph.D, Gye Young Park, M.D. Division of Pulmonary, Critical Care, Sleep and Allergy, University of Illinois at Chicago, 840 S. Wood St. CSB-920N, Chicago, IL 60612, USA. Email: hmoon22@uic.edu, parkgy@uic.edu,

Acknowledgments

We thank all the support from the Research Resource Center (Biophysics Core, Research Histology and Tissue Imaging Core, Flow Cytometry Core) at the University of Illinois at Chicago. This work was supported by NIH grant R01HL126852, Dr. Ralph and Marian Falk Medical Research Trust Bank of American, N.A., Trustee and Respiratory Health Association Grant (RHA2016-01-Lung cancer) (to G.Y.P.) and in part by NIH grants R01 HL137224 (to J.W.C.).

Abstract

Background: A new approach targeting aeroallergen sensing in the early events of mucosal immunity could have greater benefit. The CSF1-CSF1R pathway has a critical role in trafficking allergens to regional lymph nodes through activating dendritic cells. Intervention in this pathway could prevent allergen sensitization and subsequent Th2 allergic inflammation.

Objective: To examine the therapeutic effectiveness of CSF1 and CSF1R inhibition for blocking the dendritic cell function of sensing aeroallerens

Methods: We adopted a model of chronic asthma induced by a panel of three naturally occurring allergens and novel delivery system of CSF1R inhibitor encapsulated nanoprobe

This article is protected by copyright. All rights reserved.

Results: Selective depletion of CSF1 in airway epithelial cells abolished the production of allergen-reactive IgE, resulting in prevention of new asthma development as well as reversal of established allergic lung inflammation. CDPL-GW nanoprobe containing GW2580, a selective CSF1R inhibitor, showed favorable pharmacokinetics for inhalational treatment and intranasal insufflation delivery of CDPL-GW nanoprobe ameliorated asthma pathologies including allergen-specific serum IgE production, allergic lung and airway inflammation and airway hyper-responsiveness (AHR) with minimal pulmonary adverse reaction.

Conclusion: The inhibition of the CSF1-CSF1R signaling pathway effectively suppresses sensitization to aeroallergens and consequent allergic lung inflammation in a murine model of chronic asthma. CSF1R inhibition is a promising new target for the treatment of allergic asthma.

Key words

Airway epithelial cells, CSF1, CSF1R, chronic inflammation, dendritic cells, airway remodeling, asthma therapy

INTRODUCTION

Despite current standard medical treatment, a large number of patients with asthma remain symptomatic with long-term disabilities. There is a desperate need for developing a new treatment strategy for asthma. The events at the mucosal layer of airways are crucial to driving the development of Th2 immune responses. We now better understand the mechanisms by which Th2 immune-mediated allergic inflammation is initiated at the airway mucosa [1,2]. A therapeutic strategy targeting the early initial events of the mucosal immune reaction against aeroallergens could have greater therapeutic benefits because it could abolish all of the subsequent IgE- and Th2-mediated aspects of allergic inflammation in the lung.

This article is protected by copyright. All rights reserved.

Accepted Article

Asthma is a chronic airway disease consisting of atopic or non-atopic asthma. In atopic asthma, people become asthmatic through the process of '*sensitization*' against specific allergen(s) such as house dust mite and pollens. Once sensitized, individuals will develop airway inflammation and shortness of breath with re-exposure to the sensitizing allergen. Therapies targeting allergen sensitization have shown efficacy in controlling asthma [3,4]. The sensitization process for aeroallergens is mainly carried out by two major cell types, airway epithelial cells and dendritic cells.

Airway epithelial cells (AECs) are a gateway for sensing aeroallergens through first direct contact with inhaled particles [5]. Pattern recognition receptors including toll like receptors of AECs are required to recognize allergens and produce subsequent allergic inflammatory signals. Upon being activated by aeroallergens, AECs produce cytokines (TSLP, IL-1α and IL-33), chemokines (CCL2 and CCL20) and endogenous danger signals (ATP and uric acid) toward the basal side as well as luminal side and alter the micro-environmental milieu to activate innate immune cells [6]. AECs secrete innate cytokines which have a critical role in recruiting immune cells and skewing the immune reaction towards a predominant Th2 pattern [2]. On the luminal side, we and others have shown that AECs secreted chemokines into the alveolar space, recruiting monocyte-derived alveolar macrophages upon allergen challenge [7,8]. These findings indicate that AECs regulate the micro-environmental milieu of the airway in favor of allergic inflammation in response to aeroallergens.

During the sensitization, dendritic cells (DCs) take up and process the "invading" allergen and migrate to the regional lymph nodes (LNs), resulting in the establishment of allergen-specific Th2 memory. DCs form an essential interface between this innate and adaptive immunity, and play a key role in primary sensitization and the production of antigen-specific IgE [1]. DCs traffic inhaled allergens to the LNs where they launch an antigen-specific adaptive immune response involving T and B cells [9]. Conventional DCs (cDCs) play a key role in antigen presentation in various types of inflammation. cDCs express higher CCR7 which is involved in activation and homing of DCs to lymph nodes. In both human and

This article is protected by copyright. All rights reserved.

Accepted Article

mouse, two main distinct subsets of cDC, cDC1 and cDC2, possess unique characteristics and properties. cDC2 strongly depend on IRF4 and express multiple pattern recognition receptors, whereas cDC1 depend on IRF8 and activate CD8+ T cells. Especially, cDC2 have a critical role in MHC class 2-dependent antigen presentation and are more effective carriers of allergen to the regional LNs in animal models of asthma [10].

However, it has not been fully elucidated how AECs and DCs interact in the process of sensing aeroallergens. We recently reported that AECs and DCs cooperate to facilitate allergen sensitization [11]. We found that AECs secrete CSF1 into the alveolar space in response to aeroallergen. CSF1 was markedly elevated in the BAL fluids of patients with asthma after being challenged with a sensitizing allergen via bronchoscopy. With the relevant animal models, we determined that AECs are the primary source of CSF1 in BAL fluid. We observed that the epithelial-secreted CSF1 activated DCs, particularly cDC2, and facilitated mobilization to regional LNs by regulating the DC expression of CCR7, a homing chemokine receptor to LNs [11]. This is the earliest event in the mucosal immune response to aeroallergen, but also occurs as a memory response that sustains asthmatic airway disease. Blocking this process could abolish sensitization to allergens and subsequent allergic inflammation upon repeated allergen exposure.

Here, we show the effectiveness of blocking CSF1 and its receptor (CSF1R) in asthma treatment. To this end, we utilized GW2580, a selective CSF1R inhibitor, which previously showed excellent pharmacokinetics [11]. To ensure scientific rigor, we employed a robust chronic mouse model of allergic lung and airway inflammation with naturally occurring allergens. The frequently used acute mouse asthma models have limitations because they do not recapitulate the nature of human asthma as a chronic airway inflammatory disease. To develop a model that allows study of the effects of treatment on long-lasting features of asthma, e.g. airway remodeling, while avoiding the acute effects of allergen challenge, we adopted a chronic triple allergen DRA (dust mite, ragweed and *Aspergillus)* asthma model as previously reported with minor modifications [12]. This model has many of the immunologic

This article is protected by copyright. All rights reserved.

Accepted Article

and pathologic features of human asthma with continued but decreased eosinophil infiltration and prominent airway remodeling.

Materials and Methods

Mice

C57BL/6, *Scgb1a1-CreERT* (stock# 016225), *Irf4*$^{fl/fl}$ (stock# 009380) and MAFIA (stock #005070) mice were purchased from Jackson Laboratory (Bar Harbor, ME). *Scgb1a1-creERT;Csf1*$^{fl/fl}$ *and Csf1r-creERT;Irf4*$^{fl/fl}$ were generated as described previously [11]. Mice were bred in a specific pathogen-free facility maintained by the University of Illinois at Chicago. All mouse experiments were approved by the Institutional Animal Care and Use Committee of University of Illinois at Chicago. Age & sex-matched 7 to 10-week-old mice were used for experiments.

DRA-induced chronic asthma model

We used the previously described DRA-induced asthma model with minor modification [12]. In brief, mice were subject to the DRA mixture comprised of house dust mite, ragweed and *Aspergillus* (5, 50, 5 µg/mouse, respectively) twice a week via intranasal insufflation for 8 weeks. The mice were then rested for 3 weeks before collecting samples at week 11. To deplete the target genes in the experiments containing *Scgb1a1-creERT; Csf1*$^{f/f}$ (CSF1$^{\Delta AEC}$) and *Csf1r-creERT; Irf4*$^{fl/fl}$ (IRF4$^{\Delta APC}$) strains, we administered tamoxifen (Tm, 75mg/kg, Sigma-Aldrich, St. Louis, MO) via oral gavage for 5 consecutive days, according to the schedules depicted in Results.

Ex-vivo DRA antigen recall assay.

LNs were obtained from the mediastinum of the mice subjected to the DRA-induced allergic lung models. A single cell suspension was made from the LNs and a total of 4x10^6 cells/ml were plated in 24-well plates. For stimulation with the sensitizing allergens, the cells were

This article is protected by copyright. All rights reserved.

Accepted Article

treated with or without DRA (house dust mite, ragweed, and *Aspergillus*; 10, 100, 10 µg/ml, respectively) for 3 days. Cells were spun down and the supernatant used for ELISA.

Morphometric analysis and digital pathology

We used the Genie System (Aperio Technologies, Vista, CA, US), a tool for automated classification and quantitation of tissue inflammation in whole slide images, as described previously [13]. In this system, users identify the categories of tissue they want to quantify by outlining regions of interest that are examples of the tissue classes to be analyzed. We automatically quantified lung pathology over entire lung fields by categorizing them into four types: areas of normal lung parenchyma, airway, void space (such as airway lumen) and inflammation. The pathologist doing the analysis was blinded to the experimental groups.

Statistical Analysis

Student t or Mann-Whitney U test was used for two group comparisons and ANOVA was used for comparing multiple groups. Continuous variable distributions were tested for normality using Kolmogorov-Smirnov (K-S) and Shapiro–Wilk (S-W) test. SPSS 24.0 (SPSS Inc.; Chicago, IL, USA) were used for tests of normality.

Continuous variables (of which all were normally distributed) were compared between the different groups using one-way ANOVA tests in the case of homogeneity of variance between groups. If the rule of homogeneity of variance between groups was violated (K-S or S-W test $p<0.05$), Kruskal-Wallis test was performed. Descriptive statistics were expressed as mean value ± standard error of the mean (SEM) for continuous data and a p-value less than 0.05 was considered to be statistically significant. Each dot represents a single measurement of the parameters and the bar on the graph presents mean ± SEM. All analyses were conducted using Prism, GraphPad Software (La Jolla, CA).

This article is protected by copyright. All rights reserved.

Accepted Article

RESULTS

CSF1 and CSF1R$^+$cDCs are highly enriched in the BAL fluid of the chronic DRA-induced murine model of asthma.

To recapitulate the chronic inflammatory phenotype of human asthma, we adopted a chronic DRA-induced murine model of asthma as described in Methods (hereafter, the chronic DRA model) (Fig .1A left panel) [11,12]. Unlike the acute transient asthma models, eosinophilia in lung and BAL fluid was rarely seen in the chronic DRA model. Instead, the majority of BAL cells consisted of lymphocytes and macrophages and the characteristics of chronic airway inflammation and airway remodeling are well demonstrated in this model (Fig. 2D). Since AECs secrete CSF1 into the alveolar space in response to allergen exposure [11], we examined how chronic DRA exposure affects BAL CSF1 concentration. BAL CSF1 was promptly increased and peaked at week 6, whereas BAL CSF2 (GM-CSF) remained unchanged until week 6, when it began to rise (Fig.1A right panel). Conventional DCs were gated as lineage (CD3, B220, NK1.1, F4/80, CD64)$^-$CD45$^+$CD11c$^+$MHCII$^+$ and further defined either CD24^{high} for cDC1 or CD172a^{high} for cDC2 (Fig. S1A). In steady state, CSF1R positive cells were highly populated in the respiratory system, whereas their numbers were low in blood and pre-cDCs (Fig. S1B). Next, mice were subject to the chronic DRA model and the cDC2s were rapidly increased over the course of the chronic DRA model, but cDC1s were delayed until week 6. Because CSF1R$^+$ cDC2 play critical role in allergen sensitization (10), we further analyzed CSF1R$^+$ cDCs in the BAL fluids. Chronic DRA exposure induced an earlier and higher increase in CSF1R$^+$ cDC2 than that of CSF1R$^+$ cDC1 (Fig. 1B). Total and DRA-reactive serum IgE levels were also progressively increased, indicating that allergen sensitization has been intensified by repeated exposure to the allergens (Fig. 1C).

This article is protected by copyright. All rights reserved.

AEC-derived CSF1 is necessary for development of chronic allergic lung inflammation and airway remodeling.

To test whether CSF1 secreted by AECs is required for establishing chronic allergic inflammation and airway remodeling, we used the *Scgb1a1-creERT;Csf1*$^{fl/fl}$ (hereafter CSF1$^{\Delta AEC}$) mice which are the inducible knock-out mice of CSF1 selectively in AECs by tamoxifen (Tm) injection [11]. First, we measured the duration of CSF1 depletion by one single cycle (consisting of 5 consecutive days) of Tm ingestion. The CSF1 depletion in AECs and BAL fluids continued up to 4 weeks by one cycle of oral Tm (Fig. S2). Therefore, tamoxifen was administered every 4 weeks during the chronic DRA model (Fig. 2B). CSF1 in BAL was increased about 2-3 fold in the chronic DRA group (Veh_DRA), compared to the sham-treated or only tamoxifen groups (Veh_Veh, Tm_Veh), but tamoxifen treatment abolished the increase of CSF1 (Tm_DRA) (Fig. 2B). We previously reported that CSF1 has a critical role in allergen sensitization and IgE production by facilitating DC mobilization [11]. In the chronic DRA model, blocking the AEC secretion of CSF1 significantly reduced total and DRA-reactive serum IgE production (Fig. 2C) and abrogated the subsequent allergic lung inflammation, inflammatory cell infiltration, Th2 cytokine production and airway remodeling, including goblet cell metaplasia, collagen deposition and smooth muscle hypertrophy (Fig. 2D-I).

CSF1 depletion reverses established chronic allergic inflammation and airway remodeling, and suppresses Th2 memory responses.

To ensure relevance to treatment of human asthma, we created a model in which CSF1 depletion took place after the allergic lung inflammation had been fully established (Fig. 3A). In this model, oral Tm ingestion was given for one cycle at week 6 of the chronic DRA model. The one cycle of oral Tm treatment resulted in significantly decreased BAL CSF1 (Fig. 3B). The late depletion of CSF1 in the chronic DRA model was able to reverse the allergen sensitization (serum IgE), inflammatory cell infiltration, allergic lung inflammation and goblet cell metaplasia (Fig. 3C-F). A single cell suspension was made from the LNs obtained from

This article is protected by copyright. All rights reserved.

Accepted Article

the mice subjected to the above model and used for the *ex-vivo* DRA antigen recall assay as described in Methods. IL-4 and IL-13 secretion were boosted by re-challenge with DRA, but blunted in the cells obtained from the CSF1-depleted mice (Fig. 3G), indicating that the Th2 memory response was significantly reduced in CSF1-depleted micewithoutaffecting IL-17 and IFN-γ secretion by DRA re-stimulation.

IRF4$^+$ CSF1R$^+$ cells are required for Th2 memory in the secondary LNs of the chronic DRA model.

We have shown that cDC2 play a critical role in CSF1-dependent allergen sensitization [11]. Since there is no mouse strain in which cDC2 development is selectively ablated [14], we used *Csf1r-creERT;Irf4$^{fl/fl}$* (hereafter IRF4$^{\Delta APC}$) for a cDC2 targeted experiment [11]. Because IRF4 is required for cDC2 development and function, but not for cDC1 [15], and *Csf1r* expressing macrophages are not engaged in antigen trafficking to LNs, this mouse could be used for targeting cDC2 function in the experimental model of allergen sensitization [11]. The mice were subjected to the chronic DRA model as depicted in Figure 4A. In these two models, the allergic inflammation was established first, and then Tm administered to deplete the CSF1R$^+$ IRF4$^+$ cells at either week 2 (Tm2) or 6 (Tm6). Despite the presence of sufficient CSF1 in BAL fluid (Fig. 4B), the depletion of CSF1R$^+$IRF4$^+$ cells resulted in reduction of inflammatory cell infiltration and total and DRA-reactive serum IgE production, and the attenuation of lung inflammation and goblet cell metaplasia, although the Tm6 group showed only modest effects (Fig. 4C-F). The *ex-vivo* DRA antigen recall assay showed that the depletion of CSF1R$^+$ IRF4$^+$ blocked the production of IL-4 and IL-13 by DRA re-stimulation in both Tm2 and Tm6 treatment groups, whereas IL-17 production remained intact in the Tm6 group, while samples from the Tm2 group showed partial reduction (Fig. 4G). Collectively, these data indicate that CSF1R$^+$cDC2 are required for the formation of Th2 memory cells, indicating that interfering with cDC2 function should be beneficial for treating Th2-immune mediated diseases.

This article is protected by copyright. All rights reserved.

Nanoprobe carrying a CSF1R inhibitor blocks cDC2 migration and allergen sensitization.

Selective CSF1R inhibitors have been used in continuing clinical trials for cancer treatment with minimal adverse effects [16,17]. GW2580, a CSF1R inhibitor, showed excellent binding affinity to human CSF1R recombinant protein [11]. Simulation protein structure modeling indicated that GW2580 interacts with two critical intracellular tyrosine residues (Y546 and Y665) of the kinase domain of CSF1R (Fig. S3). Further, we have demonstrated that systemic administration of GW 2580 effectively blocked cDC2 migration to regional LNs [11]. The inhalational route is preferred for asthma treatment because it can deliver a compound effectively to the target organ and minimize systemic adverse effects. For an inhalational delivery, we generated a CPDL-encapsulated nanoprobe containing CSF1R inhibitor using a previously described method [18]. CDPL (β-, a synonym of β-cyclodextrins and amine of EPL, yclo**d**extrins and amine of E**PL**) nanoprobe increase the chemical stability and bioavailability of guest molecules to ensure site-specific delivery of lipophilic GW2580 to the lung without sticking to other tissues [19]. Each CPDL nanoprobe carries four molecules of GW2580 as well as a ZW800-1 fluorophore (CDPL-GW) (Fig. 5A). As expected, intranasal delivery of CDPL-GW had good lung deposition (Fig. S4). Measurements by NanoSight (Solisbury, U.K.) indicated that most of the CPDL nanoprobe were less than 100nm (Fig. S5). Next, we analyzed the cellular distribution of two different doses of CDPL-GW (1ng and 100 ng/mouse) via intranasal insufflation to the lung (Fig. S6). Neutrophils, DCs and alveolar macrophages (AMs) were the major cells that took up the particles. To optimize the dose of CDPL-GW for inhibiting DC migration in lung, the mice were subjected to DRA challenge for 5 days with increasing dose of CDPL-GW (from 1pg to 1ng/mouse) and the samples were collected on day 5 (Fig. 5B). Total BAL cells were increased by DRA challenge, but suppressed by CDPL-GW in a dose-dependent manner and BAL eosinophil counts and serum IgE concentrations were also markedly reduced by 1ng/mouse of CDPL-GW (Fig. 5B-C). However, there was no significant apoptotic death of AMs or increases in BAL total protein

This article is protected by copyright. All rights reserved.

Accepted Article

or albumin concentration by CDPL-GW treatment (Fig. 5B & S7). To further characterize the effects of CDPL-GW on DCs, we evaluated the number of migratory DCs ($CD45^+lin^-$ $CD11c^+MHCII^+CCR7^+$) in regional LNs. CDPL-GW suppressed migratory cDC2 in a dose-dependent manner (Fig. 5D). From these data, we determined that 1ng of CDPL-GW/mouse (equivalent to 80,000 nanoprobe) as the therapeutic dose for the next experiment.

Nanoprobe carrying CSF1R inhibitor abolish chronic allergic lung inflammation in the DRA model. To measure the efficacy of intranasal CDPL-GW treatment for chronic allergic inflammation, we performed three different experiments as depicted in figure S8A. In these experiments, CDPL-GW intranasal treatment was started at three different time points, week 3, 5 and 7, in the chronic DRA model, during the repeated DRA exposures until week 8. After 3 weeks of rest, the mice were analyzed at week 11. Intranasal CDPL-GW treatment in all three experiments effectively attenuated asthma pathologies including airway inflammatory cell recruitment, total and DRA-reactive serum IgE, BAL Th2 cytokines, lung tissue inflammation and goblet cell metaplasia, compared to the sham treated group, although the CDPL-GW 7wk group had only modest effects (Fig. 6A-E). There was no change in the BAL concentrations of total protein and albumin (Fig. S8B). CDPL-GW treatment effectively inhibited Th2 memory cell formation in the secondary LNs, although the CDPL-GW 7wk group did not reach statistical significance (Fig. 6F). All three CDPL-GW treated groups showed reduced bronchial hyper-responsiveness, compared to the sham-treated chronic DRA group (Fig. 6G).

Accepted Article

This article is protected by copyright. All rights reserved.

Accepted Article

DISCUSSION

Our study highlights the effects of blocking or minimizing allergen sensitization on development and exacerbation of asthma pathologies, respectively. Earlier clinical studies indicate that sensitization to environmental allergens and excessive production of serum IgE precedes manifestation of allergic asthma in the early childhood [20,21]. In the cohort of a large group of newborns, the prevalence of asthma was significantly higher among ever-allergic sensitized children compared to never-sensitized ones [22]. These data strongly suggest a causal relationship between allergen sensitization and development of clinical asthma. Therapies to reduce allergen sensitization have been tried using many different approaches. Allergen immunotherapy with allergen extracts is able to lower allergen-specific IgE as well as increase specific IgG4 levels, resulting in a robust long-lasting effect on seasonal rhinitis and peanut allergy [23-25]. Sensitization to allergen(s) occurs not only in the development of new asthma, but also in the exacerbation of established asthma. We have shown that serum IgE is increased by re-exposure to the sensitizing allergen in the mouse DRA model of allergic asthma [11]. Intervening in the continuing sensitization process has been shown to prevent asthma exacerbations in the patients already sensitized. For example, IgE-targeted treatment with omalizumab, a humanized monoclonal anti-IgE antibody, showed a significant benefit in controlling asthma exacerbations in inner city children who were already sensitized to cockroach [3]. Pre-seasonal treatment with omalizumab was also effective in controlling seasonal exacerbations in poorly controlled asthmatics [4]. Here, we examined three animal models to validate the effect of intervening in the CSF1-CSF1R pathway for preventing both the development of new allergic asthma and reversing fully established allergic lung inflammation. In all three models, our data showed that blocking the CSF1-CSF1R pathway effectively abolished the sensitization process (reducing both total and allergen-reactive serum IgE) and suppressed subsequent allergic lung inflammation. These data support the concept that blocking the allergen sensitization process can effectively prevent the

This article is protected by copyright. All rights reserved.

subsequent Th2 allergic inflammatory process regardless of the onset of allergic inflammation, and could be used as a maintenance therapy for chronic asthma.

Among DC subsets, cDC2 have been shown to play an essential role in antigen presentation in allergic lung inflammation [10,11,26]. Our data show a marked surge of cDC2 in BAL fluid in the DRA asthma model [11]. However, it is not fully understood how alveolar cDC2 are regulated in allergic inflammation. Recently, we reported that the CSF1-CSF1R pathway is critical for cDC2 activation through their homing to regional LNs and establishing subsequent Th2 immune reactions in response to inhaled allergens. We have shown that the binding of AEC-derived CSF1 to its receptor on cDC2 facilitates expression of the chemokine receptor, CCR7 [11]. Based on this scientific premise, here we rigorously examined whether intervening in this pathway would be beneficial for controlling both new and established allergic lung inflammation. To examine the therapeutic effectiveness, we adopted a mouse model of chronic asthma [12]. Unlike the transient acute models of allergic asthma, this model shows marked inflammatory cell infiltration and prominent airway remodeling, including structural alterations, prominent tissue fibrosis and chronic inflammation, albeit with decreased eosinophilia (Figure 2). This model is better suited for evaluating the long term effects of asthma therapeutics on well-established asthma pathologies, in this case, treatment with anti-CSF1 antibodies and nanoprobe carrying a CSF1R antagonist.

CSF1 and its receptor (CSF1R) regulate the functions of myeloid lineage cells that play key roles in innate immune responses [27]. CSF1R is comprised of five extracellular immunoglobulin domains, a transmembrane domain, and two intracellular domains. The *CSF1R* gene is evolutionally well conserved and has high sequence homology between species. Especially, the intracellular domains of human and murine CSF1R genes are identical (NCBI HomologGene). In humans, the *CSF1R* gene is located at the chromosomal region 5q32, which is close to genes associated with genetic susceptibility to asthma including *IL-4, IL-5* and *ADRB2* [28-30]. Furthermore, it has been reported that a polymorphism of the *CSF1R* gene is associated with an increased risk for asthma in humans [31]. Upon

This article is protected by copyright. All rights reserved.

Accepted Article

binding with its ligand, CSF1, the intracellular kinase domain of CSF1R undergoes auto-phosphorylation and activates multiple downstream pathways [27]. CSF1R inhibitors bind to the tyrosine residues of the intracellular kinase domain. Our structure-based simulation shows that the CSF1R inhibitor, GW2580, binds two tyrosine residues (Y546 and Y665) (Figure E3). Further studies are necessary to delineate the effect of GW2580 binding to CSF1R and modulation of downstream signaling pathways associated with allergic airway responses.

Systemic administration of CSF1R inhibitors as anti-cancer agents has been shown to have excellent clinical safety and good tolerance, even in patients with advanced-staged malignancies [16,17]. Here, we examined the therapeutic efficacy and potential pulmonary toxicities of locally administered CSF1R inhibitor, GW2580. Our data show a decrease in BAL eosinophil count and serum IgE level with inhalational delivery of CDPL-GW at the dose of 1 ng/mouse, which is equivalent to 8,000 nanoprobe per mouse. These data indicate that the DCs involved in allergen sensitization are highly sensitive to blockade of the CSF1-CSF1R pathway. Since not only DCs but also macrophages express CSF1R, macrophage dysfunction related to CSF1R inhibition may lead to potential adverse effects. Although not being involved in antigen presentation, AMs are a first-line of defense against inhaled foreign particles. Here, we examined the potential pulmonary toxicities of locally administered CSF1R inhibitor nanoprobe. The intranasal delivery of CDPL-GW (up to 1ng/mouse) to the airway did not increase AM cell death in terms of the number of apoptotic AMs. Various forms of pulmonary alveolar proteinosis (PAP) can develop because of impaired function of GM-CSF or its receptor (CSF2R). We examined whether CDPL-GW induced PAP in the mice, even though CSF1R is structurally different from the GM-CSF receptor and there is no known cross-reactivity between these two receptors. Our data showed that there was no increase in total protein or albumin concentrations in BAL fluid, and lung pathology showed no evidence of PAP after treatment with intranasal CDPL-GW. These data suggest that the sensitivity of the CSF1R receptor to CSF1R inhibition varies depending on the cell type. Our

This article is protected by copyright. All rights reserved.

Accepted Article

previous report showing variable expression of CSF1R among myeloid cells supports this hypothesis [11]. Of interest, blocking the CSF1-CSF1R pathway selectively inhibits Th2 memory, but Th1 and Th17 memory function remained intact, suggesting that immune defense against viral and bacterial infection may remain intact as well, although this requires further investigation. Previous reports indicate that the differentiation and survival of AMs heavily depends on GM-CSF and its receptor [32,33], suggesting that CSF1R could be dispensable for macrophages in the alveolar niche. Further study is needed to clarify the biological function of the CSF1 receptor on alveolar macrophages.

In summary, our data support the efficacy of a DC centered new treatment of asthma that targets the CSF1-CSF1R pathway to block the process of allergen sensitization. Because allergen sensitization is required not only for establishing new atopic asthma, but also for exacerbation of allergic inflammation in already established asthma, the approach of blocking the sensitization process could be used as a long term maintenance therapy for the treatment of asthma.

Accepted Article

This article is protected by copyright. All rights reserved.

Accepted Article

REFERENCES

1. Lambrecht BN, Hammad H. Biology of lung dendritic cells at the origin of asthma. *Immunity.* 2009;31(3):412-424.
2. Hammad H, Lambrecht BN. Barrier Epithelial Cells and the Control of Type 2 Immunity. *Immunity.* 2015;43(1):29-40.
3. Busse WW, Morgan WJ, Gergen PJ, et al. Randomized trial of omalizumab (anti-IgE) for asthma in inner-city children. *N Engl J Med.* 2011;364(11):1005-1015.
4. Teach SJ, Gill MA, Togias A, et al. Preseasonal treatment with either omalizumab or an inhaled corticosteroid boost to prevent fall asthma exacerbations. *J Allergy Clin Immunol.* 2015;136(6):1476-1485.
5. Lambrecht BN, Hammad H. Allergens and the airway epithelium response: gateway to allergic sensitization. *J Allergy Clin Immunol.* 2014;134(3):499-507.
6. Whitsett JA, Alenghat T. Respiratory epithelial cells orchestrate pulmonary innate immunity. *Nature immunology.* 2015;16(1):27-35.
7. Lee YG, Jeong JJ, Nyenhuis S, et al. Recruited alveolar macrophages, in response to airway epithelial-derived monocyte chemoattractant protein 1/CCl2, regulate airway inflammation and remodeling in allergic asthma. *Am J Respir Cell Mol Biol.* 2015;52(6):772-784.
8. Zaslona Z, Przybranowski S, Wilke C, et al. Resident alveolar macrophages suppress, whereas recruited monocytes promote, allergic lung inflammation in murine models of asthma. *J Immunol.* 2014;193(8):4245-4253.
9. Joffre O, Nolte MA, Sporri R, Reis e Sousa C. Inflammatory signals in dendritic cell activation and the induction of adaptive immunity. *Immunol Rev.* 2009;227(1):234-247.
10. Plantinga M, Guilliams M, Vanheerswynghels M, et al. Conventional and monocyte-derived CD11b(+) dendritic cells initiate and maintain T helper 2 cell-mediated immunity to house dust mite allergen. *Immunity.* 2013;38(2):322-335.
11. Moon H-G, Kim S-j, Jeong JJ, et al. Airway Epithelial Cell-Derived Colony Stimulating Factor-1 Promotes Allergen Sensitization. *Immunity.* 2018;49(2):275-287.e275.
12. Goplen N, Karim MZ, Liang Q, et al. Combined sensitization of mice to extracts of dust mite, ragweed, and Aspergillus species breaks through tolerance and establishes chronic features of asthma. *Journal of Allergy and Clinical Immunology.* 2009;123(4):925-932.e911.
13. Park GY, Lee YG, Berdyshev E, et al. Autotaxin production of lysophosphatidic acid mediates allergic asthmatic inflammation. *Am J Respir Crit Care Med.* 2013;188(8):928-940.
14. Anderson DA, 3rd, Murphy KM, Briseno CG. Development, Diversity, and Function of Dendritic Cells in Mouse and Human. *Cold Spring Harb Perspect Biol.* 2017.
15. Bajana S, Turner S, Paul J, Ainsua-Enrich E, Kovats S. IRF4 and IRF8 Act in CD11c+ Cells To Regulate Terminal Differentiation of Lung Tissue Dendritic Cells. *J Immunol.* 2016;196(4):1666-1677.
16. Butowski N, Colman H, De Groot JF, et al. Orally administered colony stimulating factor 1 receptor inhibitor PLX3397 in recurrent glioblastoma: an Ivy Foundation Early Phase Clinical Trials Consortium phase II study. *Neuro Oncol.* 2016;18(4):557-564.
17. Tap WD, Wainberg ZA, Anthony SP, et al. Structure-Guided Blockade of CSF1R Kinase in Tenosynovial Giant-Cell Tumor. *N Engl J Med.* 2015;373(5):428-437.
18. Kang H, Gravier J, Bao K, et al. Renal Clearable Organic Nanocarriers for Bioimaging and Drug Delivery. *Adv Mater.* 2016;28(37):8162-8168.
19. Choi HS, Ashitate Y, Lee JH, et al. Rapid translocation of nanoparticles from the lung airspaces to the body. *Nat Biotechnol.* 2010;28(12):1300-1303.
20. Hose AJ, Depner M, Illi S, et al. Latent class analysis reveals clinically relevant atopy phenotypes in 2 birth cohorts. *J Allergy Clin Immunol.* 2017;139(6):1935-1945 e1912.
21. Rhodes HL, Thomas P, Sporik R, Holgate ST, Cogswell JJ. A birth cohort study of subjects at risk of atopy: twenty-two-year follow-up of wheeze and atopic status. *Am J Respir Crit Care Med.* 2002;165(2):176-180.

This article is protected by copyright. All rights reserved.

22. Ballardini N, Bergstrom A, Wahlgren CF, et al. IgE antibodies in relation to prevalence and multimorbidity of eczema, asthma, and rhinitis from birth to adolescence. *Allergy.* 2016;71(3):342-349.
23. Durham SR, Emminger W, Kapp A, et al. SQ-standardized sublingual grass immunotherapy: confirmation of disease modification 2 years after 3 years of treatment in a randomized trial. *J Allergy Clin Immunol.* 2012;129(3):717-725 e715.
24. Durham SR, Emminger W, Kapp A, et al. Long-term clinical efficacy in grass pollen-induced rhinoconjunctivitis after treatment with SQ-standardized grass allergy immunotherapy tablet. *J Allergy Clin Immunol.* 2010;125(1):131-138 e131-137.
25. Du Toit G, Roberts G, Sayre PH, et al. Randomized trial of peanut consumption in infants at risk for peanut allergy. *N Engl J Med.* 2015;372(9):803-813.
26. Hammad H, Plantinga M, Deswarte K, et al. Inflammatory dendritic cells--not basophils--are necessary and sufficient for induction of Th2 immunity to inhaled house dust mite allergen. *J Exp Med.* 2010;207(10):2097-2111.
27. Stanley ER, Chitu V. CSF-1 receptor signaling in myeloid cells. *Cold Spring Harb Perspect Biol.* 2014;6(6).
28. Turner S, Francis B, Vijverberg S, et al. Childhood asthma exacerbations and the Arg16 beta2-receptor polymorphism: A meta-analysis stratified by treatment. *J Allergy Clin Immunol.* 2016;138(1):107-113 e105.
29. Zhu S, Chan-Yeung M, Becker AB, et al. Polymorphisms of the IL-4, TNF-alpha, and Fcepsilon RIbeta genes and the risk of allergic disorders in at-risk infants. *Am J Respir Crit Care Med.* 2000;161(5):1655-1659.
30. Sordillo JE, Kelly R, Bunyavanich S, et al. Genome-wide expression profiles identify potential targets for gene-environment interactions in asthma severity. *J Allergy Clin Immunol.* 2015;136(4):885-892 e882.
31. Shin EK, Lee SH, Cho SH, et al. Association between colony-stimulating factor 1 receptor gene polymorphisms and asthma risk. *Hum Genet.* 2010;128(3):293-302.
32. Guilliams M, Scott CL. Does niche competition determine the origin of tissue-resident macrophages? *Nat Rev Immunol.* 2017;17(7):451-460.
33. van de Laar L, Saelens W, De Prijck S, et al. Yolk Sac Macrophages, Fetal Liver, and Adult Monocytes Can Colonize an Empty Niche and Develop into Functional Tissue-Resident Macrophages. *Immunity.* 2016;44(4):755-768.

Accepted Article

This article is protected by copyright. All rights reserved.

Accepted Article

FIGURE LEGENDS

Figure 1. CSF1 and CSF1R$^+$cDCs are highly enriched in the BAL fluid of the chronic DRA model. (A) Left: Experimental scheme for the chronic DRA-induced murine model of asthma (the chronic DRA model). Right: The BAL fluids were obtained at the indicated time points and the level of CSF1 in the BAL fluids was measured by ELISA (n=4-6 mice per group). (B) By using the gating strategy as depicted in Figure E1, cDC and CSF1R$^+$cDC populations were measured in the BAL fluids over the course of the chronic DRA model. (C) The concentrations of total and DRA-reactive serum IgE were measured at the indicated time points. The DRA-reactive serum IgE is expressed as fold increase, compared to the steady state IgE level. *p<0.05, **p<0.01

Figure 2. Depletion of AEC-derived CSF1 prevents allergen sensitization and abolishes chronic allergic lung inflammation. (A) Experimental scheme for depleting AEC-derived CSF1 in the chronic DRA model using *Scgb1a1-creERT;Csf1*$^{fl/fl}$ (CSF1$^{\Delta AEC}$) mice. Tamoxifen was orally administered for 5 consecutive days (one cycle) every 4 weeks. All samples were collected at the end of week 11 (n=9-16 mice per group). (B-E) Tamoxifen alone has no effect on the BAL cytokines in the absence of DRA challenge (Tm_Veh), although lowering slightly the basal BAL CSF1 level (Figure 2B). DRA challenge induced marked increases in BAL CSF1, IL-4 and IL-13 (Veh_DRA), which were significantly reduced by Tm treatment (Tm_DRA) (2B & E). Total and DRA-reactive serum IgE concentrations were also suppressed by Tm treatment (2C). The DRA-reactive serum IgE are expressed as fold increase compared to that of the sham-treated control group (Veh_Veh). The increase in total BAL cells was suppressed by Tm treatment and the cells were mainly comprised of macrophages and lymphocytes (2D). (F) Morphometric digital pathologic analysis was performed over an entire single lung field as described in Methods. The color codes for the digital pathology indicate the following: green-inflammatory cells; yellow-area of the airway; brown-void space. The area of inflammation was markedly reduced by Tm treatment. The scale bars are 5 mm in middle and 500 μm in right panels. (G-I) Periodic acid Schiff (PAS)

This article is protected by copyright. All rights reserved.

staining for goblet cells and immunofluorescence staining with anti-collagen and anti-α-smooth muscle actin antibodies were compared between the Tm-treated and sham-treated DRA groups. The signals were quantified by measurement of the signals per field. Scale bars represent 200μm. *p<0.05, **p<0.01.

Figure 3. CSF1 depletion reverses established chronic allergic inflammation and airway remodeling, and suppresses Th2 memory responses in LNs. (A) Experimental scheme for depleting AEC-derived CSF1 in the chronic DRA allergic inflammation model. Tm was administered for only one cycle, at week 6 of the chronic DRA model. (n=5-8 mice per group) (B) Single treatment with Tm (DRA/Tm) at week 6 reduced the BAL CSF1 concentration. (C-F) Tm treatment in the late phase of the model was able to reverse the BAL lymphocytosis, increased serum IgE, chronic lung inflammation and goblet cell metaplasia. The scale bars in left and right of (E) and (F) are 5 mm, 500 μm and 200μm, respectively. (G) The cells from the LNs were isolated from each group, and then re-stimulated with or without DRA for 72 hours *ex-vivo* in culture. The cytokines in culture supernatants were measured. The re-stimulation with DRA increased the secretion of IL-4, IL-13, IL-17 and IFN-γ in the LN cultures. However, the group treated with Tm (DRA/Tm) showed a blunted response for IL-4 and IL-13, whereas IL-17 and IFN-γ levels remained unchanged. *p<0.05, **p<0.01.

Figure 4. IRF4^{+} CSF1R^{+} cells are required for allergen sensitization and Th2 memory in the secondary LNs. (A) Experimental scheme for depleting CSF1R^{+}IRF4^{+} antigen presenting cells in *Csf1r-cre*ERT;*Irf4*$^{fl/fl}$ (Irf4$^{\Delta APC}$) mice. Tm2 and Tm6 indicate that the Tm administration was started at weeks 2 and 6 of the chronic DRA model as depicted. (n=5-8 mice per group) (B) Depletion of CSF1R^{+}IRF4^{+} in Irf4$^{\Delta APC}$ mice had no effect on BAL CSF1 concentration. (C-F) However, depletion of CSF1R^{+}IRF4^{+} from week 2 (Tm2) resulted in a modest decrease in BAL inflammatory cells, significant reduction of total and DRA-reactive serum IgE, marked reduction of chronic lung inflammation and goblet cell metaplasia. The Tm6 group showed similar trends, but was less effective than in the Tm2 group. Left and

This article is protected by copyright. All rights reserved.

Accepted Article

middle scale bars in (E) are 5 mm and 500 μm, respectively. (G) Single cell suspensions of LNs were isolated from each group and re-stimulated with DRA for 72 hours. The cytokines in culture supernatants were measured. The re-stimulation with DRA boosted the secretion of IL-4, IL-13 and IL-17, compared to the sham-treated control. However, the Tm treated groups showed a blunted response for IL-4 and IL-13 production, whereas IL-17 secretion in the Tm 6 group was not affected by Tm treatment while the Tm2 group showed a mild decrease in IL-17 production. * $p<0.05$, ** $p<0.01$

Figure 5. CDPL-GW nanoprobe carrying CSF1R inhibitor block cDC2 migration and allergen sensitization. (A) Structure of the CDPL-GW nanoprobe which carries 4 molecules of GW2580, a selective CSF1R inhibitor and a ZW800-1 fluorescent dye. (B-C) The experimental scheme to optimize the dose of CDPL-GW. The total AM count and annexin V^+ AMs in BAL fluids were measured by flow cytometry. AMs and eosinophils in BAL fluids were identified by $CD11c^+SiglecF^+$, $CD11c^-SiglecF^+$ respectively. DRA challenge induced increases in BAL AMs and eosinophils, which was inhibited by the CDPL-GW treatment in a dose dependent manner. However, there was no change in the proportion of annexin V^+ cells up to 1ng (=1000pg) of CDPL-GW /mouse which was a sufficient dose to suppress the BAL eosinophil recruitment and total serum IgE rise (n=4-5 mice per group). (D) Migratory DCs (defined by $CD45^+lineage^-CD11c^+MHCII^+CCR7^+$) were measured in the single cell suspensions isolated from mediastinal LNs. The number of migratory DCs in LNs gradually declined as the dose of CDPL-GW inhibitor was increased via the intranasal route (n=4-5). * $p<0.05$

Figure 6. Intranasal delivery of CDPL-GW nanoprobe abolishes chronic allergenic lung inflammation in the DRA model. Mice were subjected to the chronic DRA model, and then treated with CDPL-GW (1ng/mouse via the *i.n*. route, twice a week) in three different designs as depicted in Figure E8. CDPL-GW 3wk indicates that the treatment with CDPL-GW was started at week 3 of the chronic DRA model and maintained until week 8 (total of 6 weeks). CDPL-GW 5wk and 7wk were done in a similar fashion. All of the measurements

This article is protected by copyright. All rights reserved.

were done at week 11. (n=5-10 mice per group) (A) Treatment with CDPL-GW markedly reduced the DRA-induced BAL cellular recruitment which was mainly comprised of macrophages and lymphocytes. (B-E) CDPL-GW treatment starting at 3 and 5 weeks of the chronic DRA model (CDPL-GW 3wk and 5wk) effectively blocked the increases in total and DRA-reactive serum IgE, BAL IL-4 and IL-5, and attenuated lung inflammation and goblet cell metaplasia. However, the CDPL-GW 7wk group showed similar trends, but differences failed to reach statistical significance in terms of DRA-reactive serum IgE, lung inflammation and goblet cell metaplasia. Scale bars represent 200μm. (F) Single cell suspensions of regional LNs were re-stimulated with DRA for 72 hours. DRA re-stimulation increased the secretion of IL-4, IL-13 and IL-17, but CDPL-GW treatment blocked these increases. However, cytokine levels from cells obtained from the CDPL-GW 7wk group did not reach statistical significance compared to those of the sham-treated DRA group, although they showed a declining trend. (G) Airway resistance was measured using increasing doses of methacholine in the sham and CDPL-GW treated groups after DRA challenge. All of the three CDPL-GW treated groups had significantly lower airway resistance compared to the sham treated chronic DRA group.

CONFLICT OF INTEREST

H.M. and G.Y.P. have filed a provisional patent application related to the submitted manuscript.

AUTHOR CONTRIBUTIONS

H.-G.M. performed the mouse and cellular experiments, analyzed data, and drafted the manuscript. S.K. assisted the mouse and cellular experiments. M.K.L performed statistical analysis. H.K. and H.S.C. provided CDPL-GW nanoprobe and conducted pharmacokinetics study. A.H. performed methacholine challenge tests. J.R. performed molecular docking

This article is protected by copyright. All rights reserved.

Accepted Article

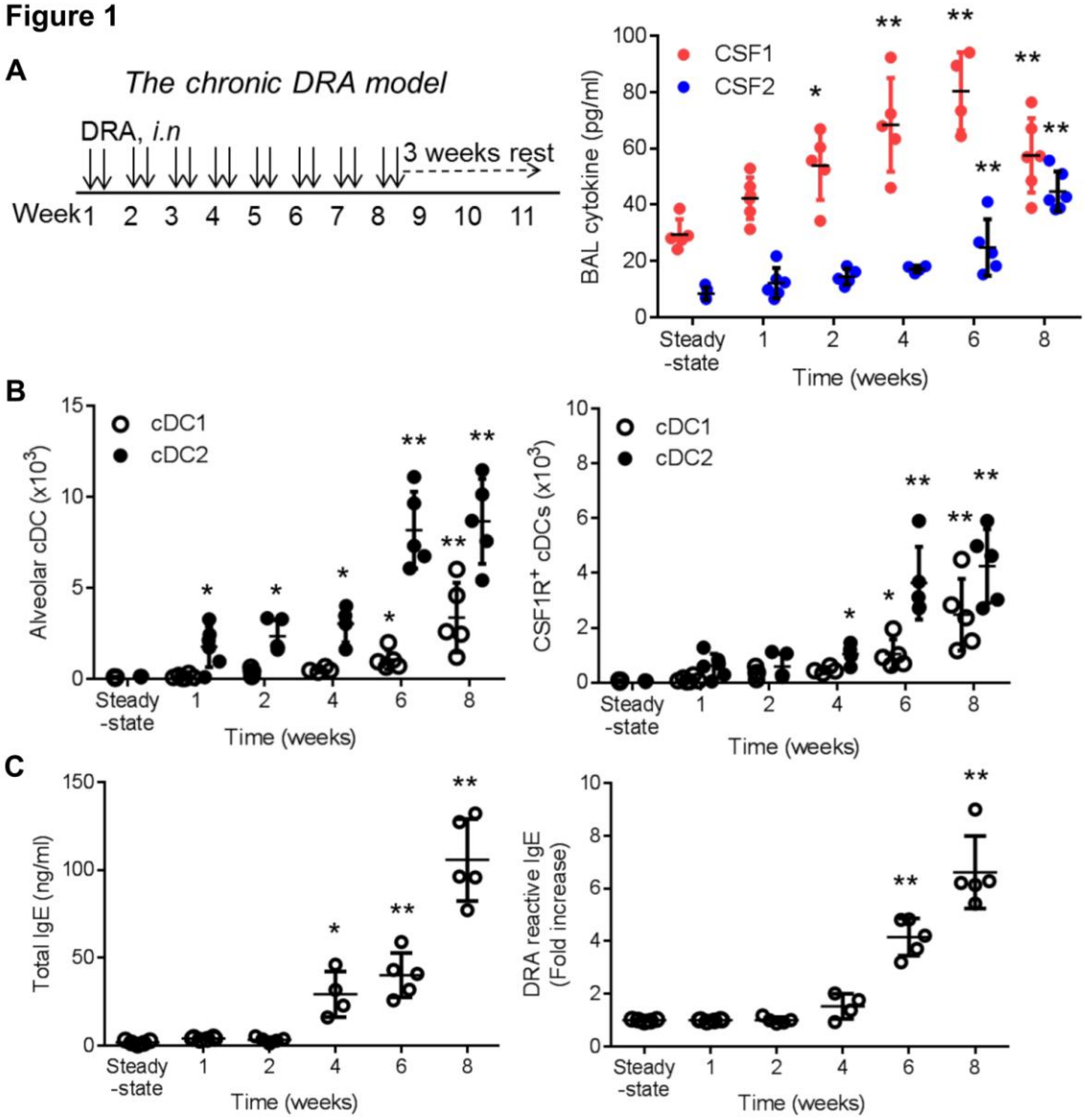
study of CSF1R kinase domain. S.J.A., V.N., and J.W.C. assisted with data analyses and edited the manuscript. G.Y.P. conceptualized and supervised the study.

Accepted Article

This article is protected by copyright. All rights reserved.

Accepted Article

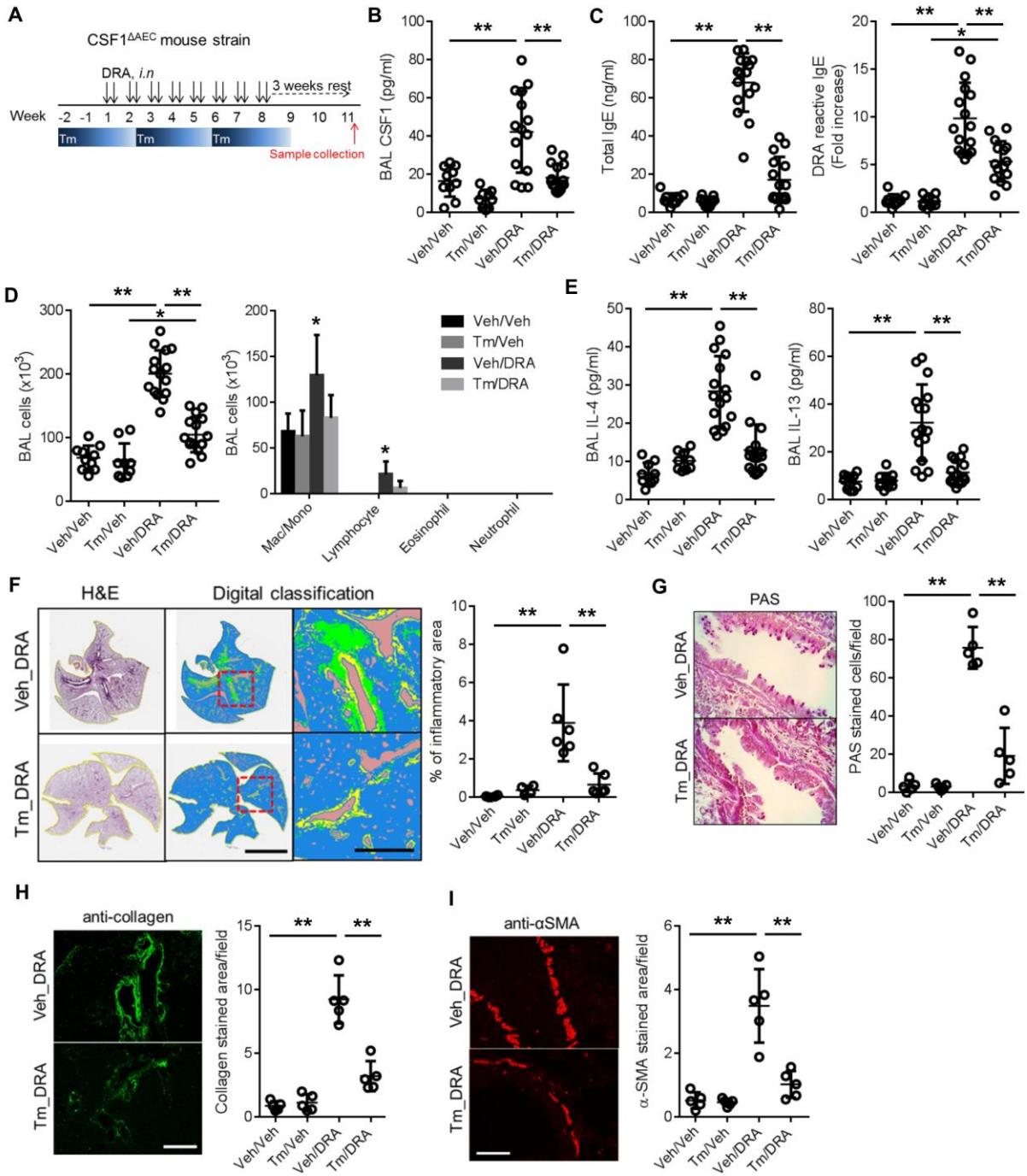
Figure 1



This article is protected by copyright. All rights reserved.

Accepted Article

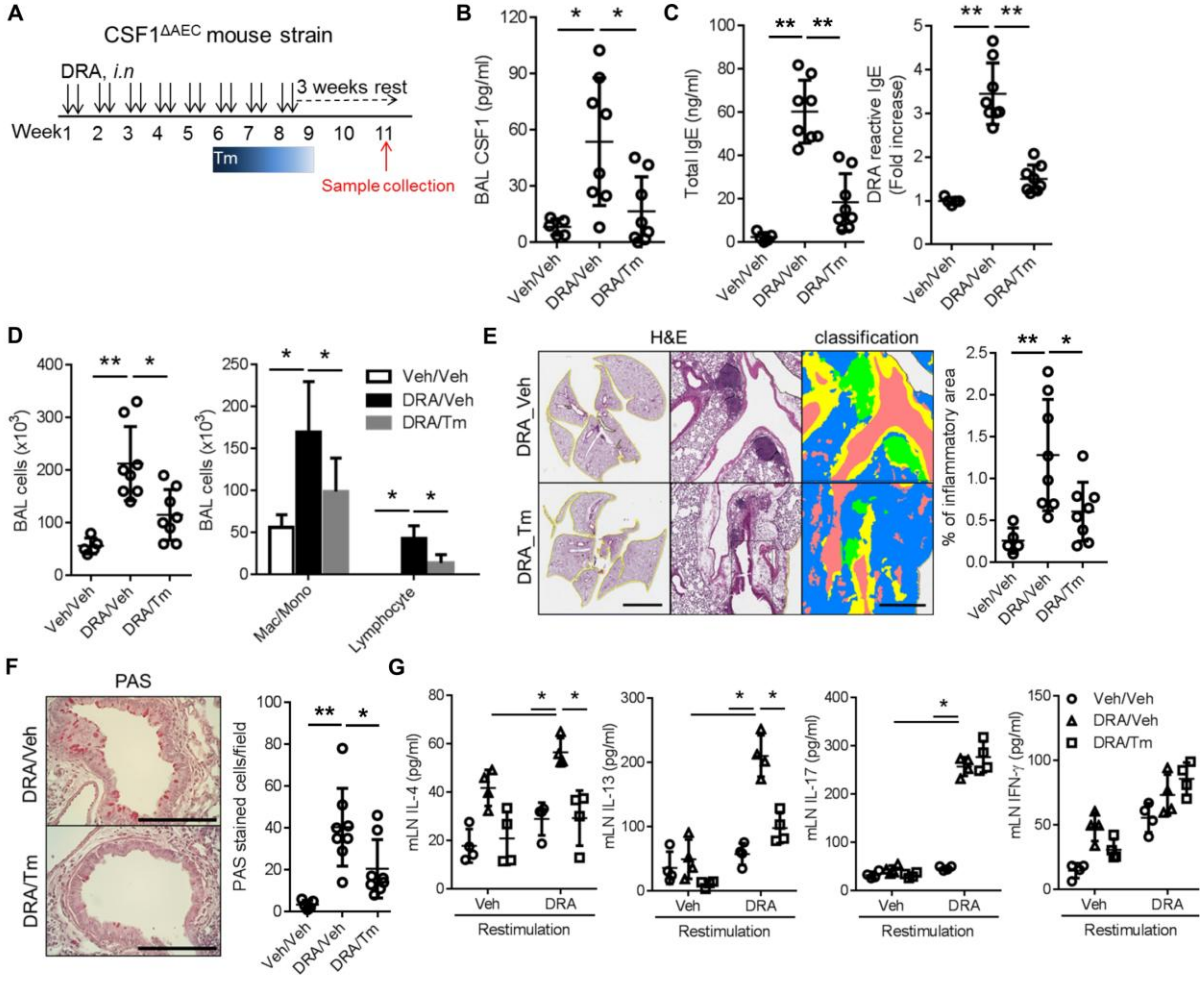
Figure 2



This article is protected by copyright. All rights reserved.

Accepted Article

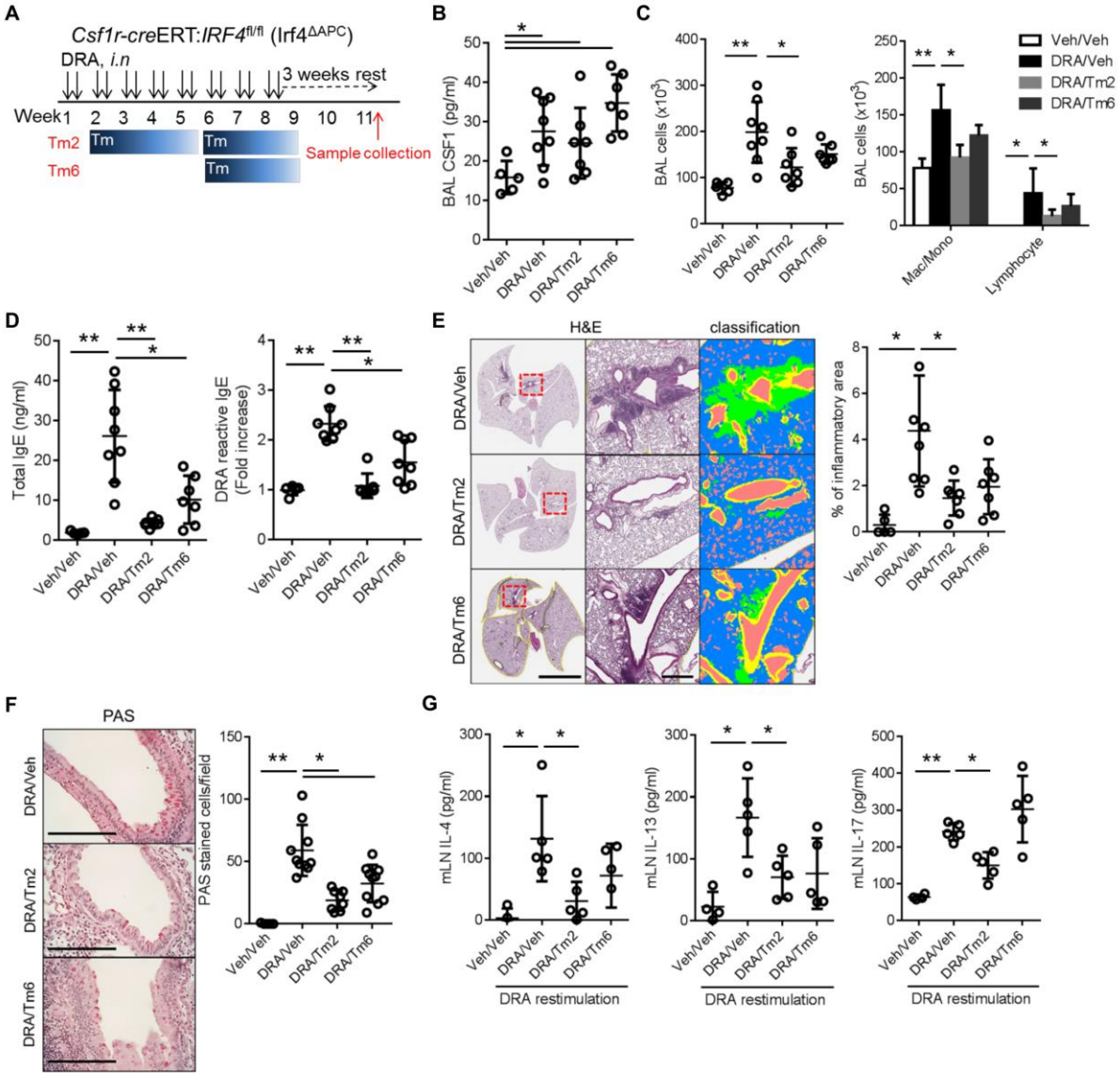
Figure 3



This article is protected by copyright. All rights reserved.

Accepted Article

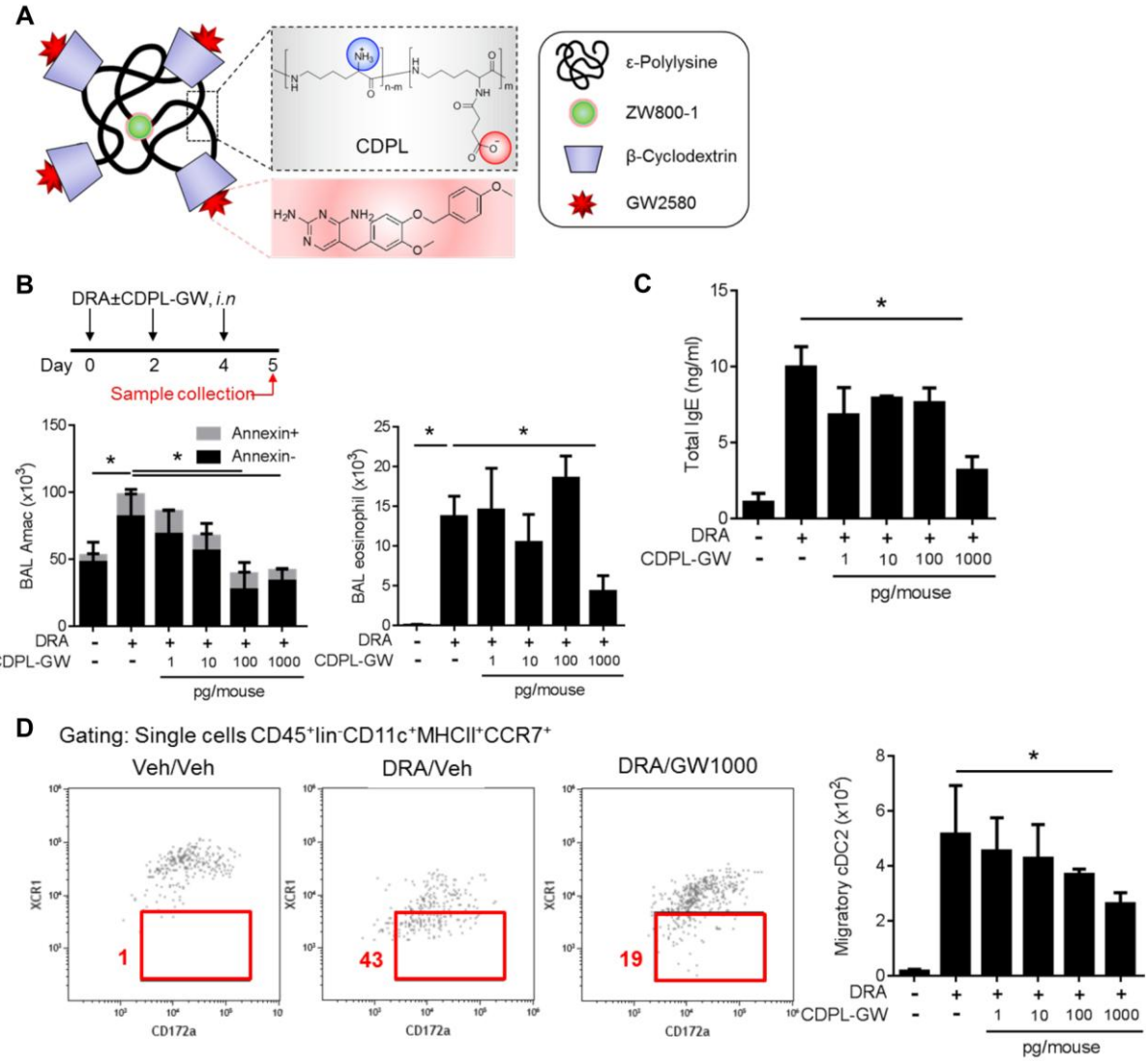
Figure 4



This article is protected by copyright. All rights reserved.

Accepted Article

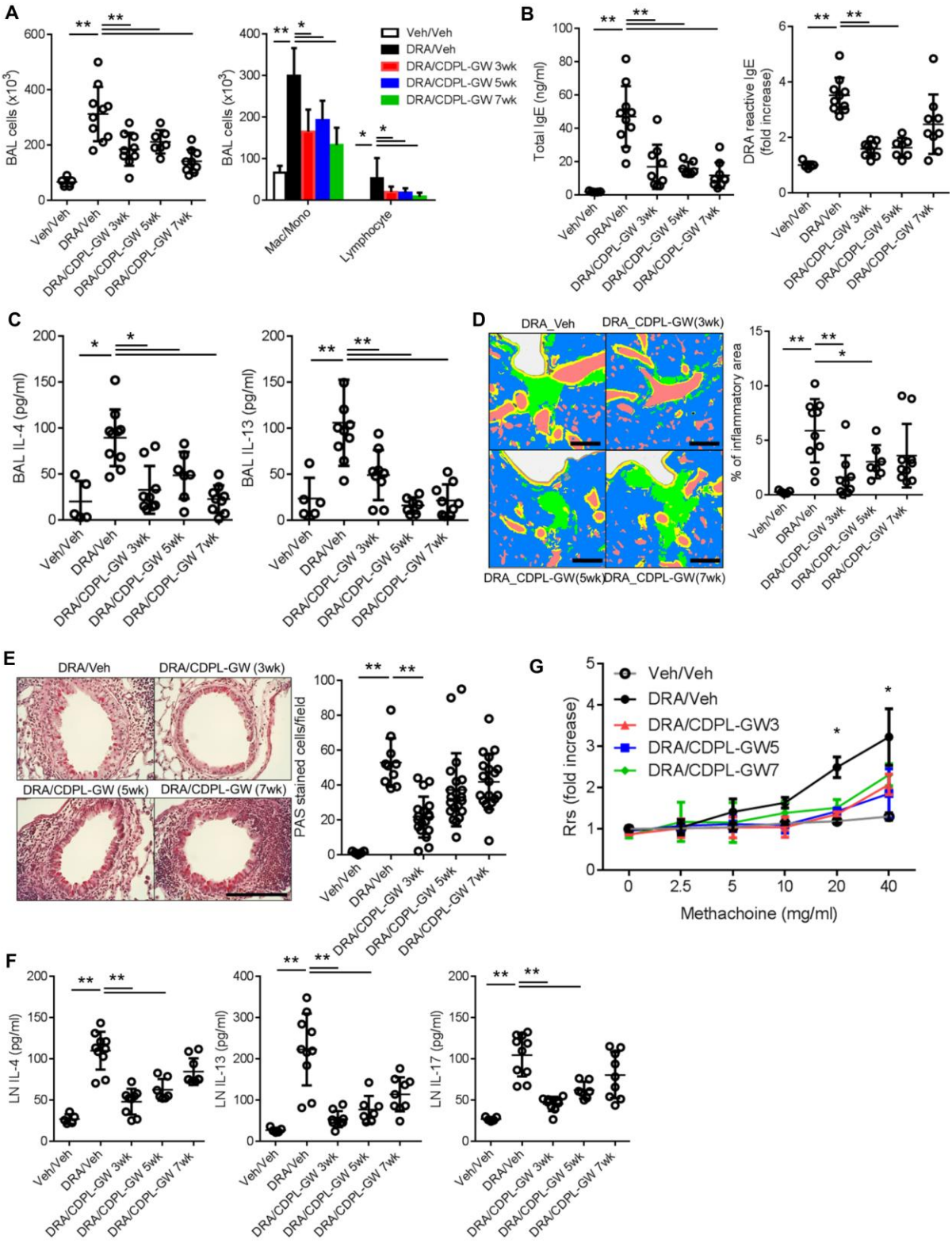
Figure 5



This article is protected by copyright. All rights reserved.

Accepted Article

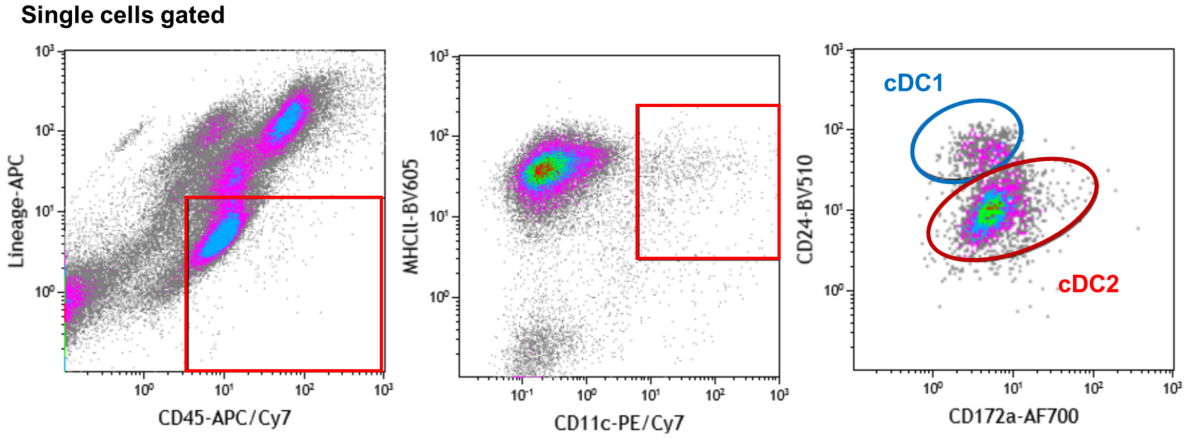
Figure 6



This article is protected by copyright. All rights reserved.

Figure S1

A


Single cells gated
Lineage-APC
CD45-APC/Cy7
MHCII-BV605
CD11c-PE/Cy7
CD24-BV510
CD172a-AF700
cDC1
cDC2

B

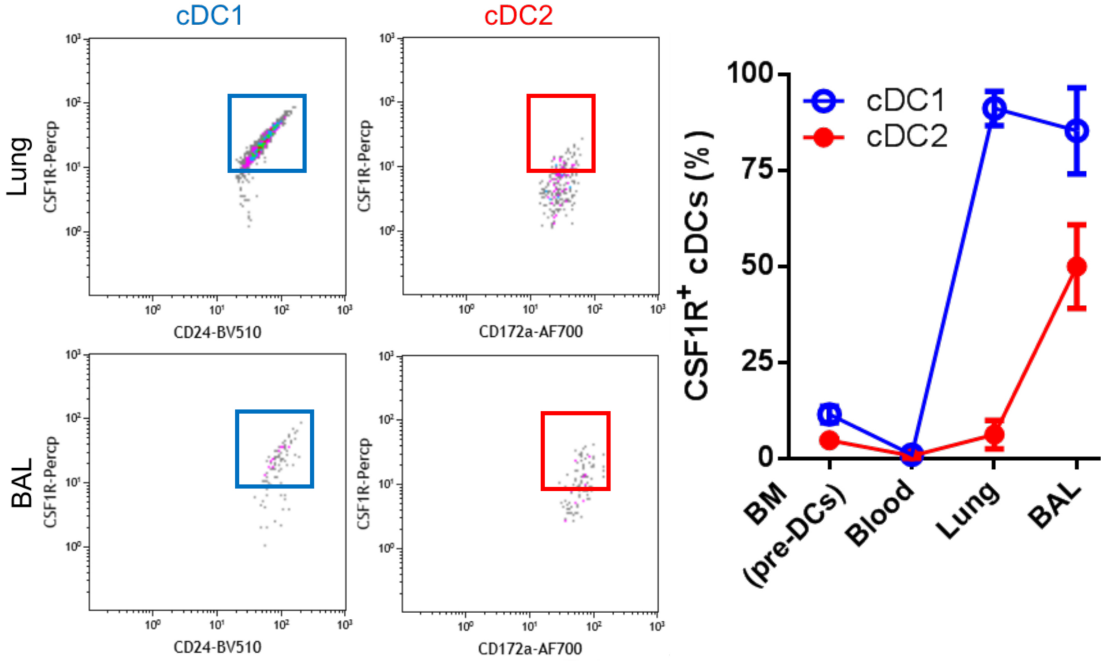
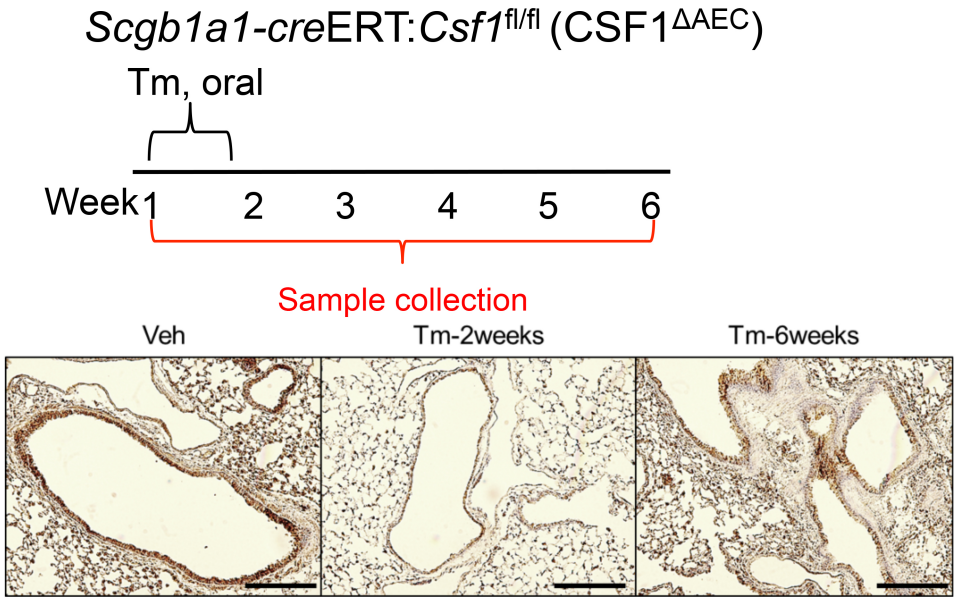

Steady state
cDC1
cDC2
Lung
BAL
CSF1R-Percp
CD24-BV510
CD172a-AF700
CSF1R+ cDCs (%)
100
75
50
25
0
BM (pre-DCs)
Blood
Lung
BAL

Figure S2


Scgb1a1-creERT:Csf1fl/fl (CSF1ΔAEC)
Tm, oral
Week 1 2 3 4 5 6
Sample collection
Veh
Tm-2weeks
Tm-6weeks

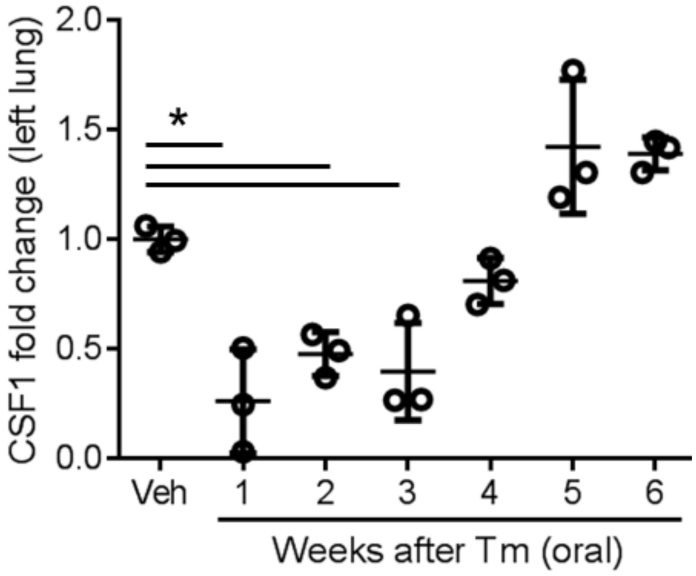

CSF1 fold change (left lung)
2.0
1.5
1.0
0.5
0.0
*
Veh 1 2 3 4 5 6
Weeks after Tm (oral)

Figure S3

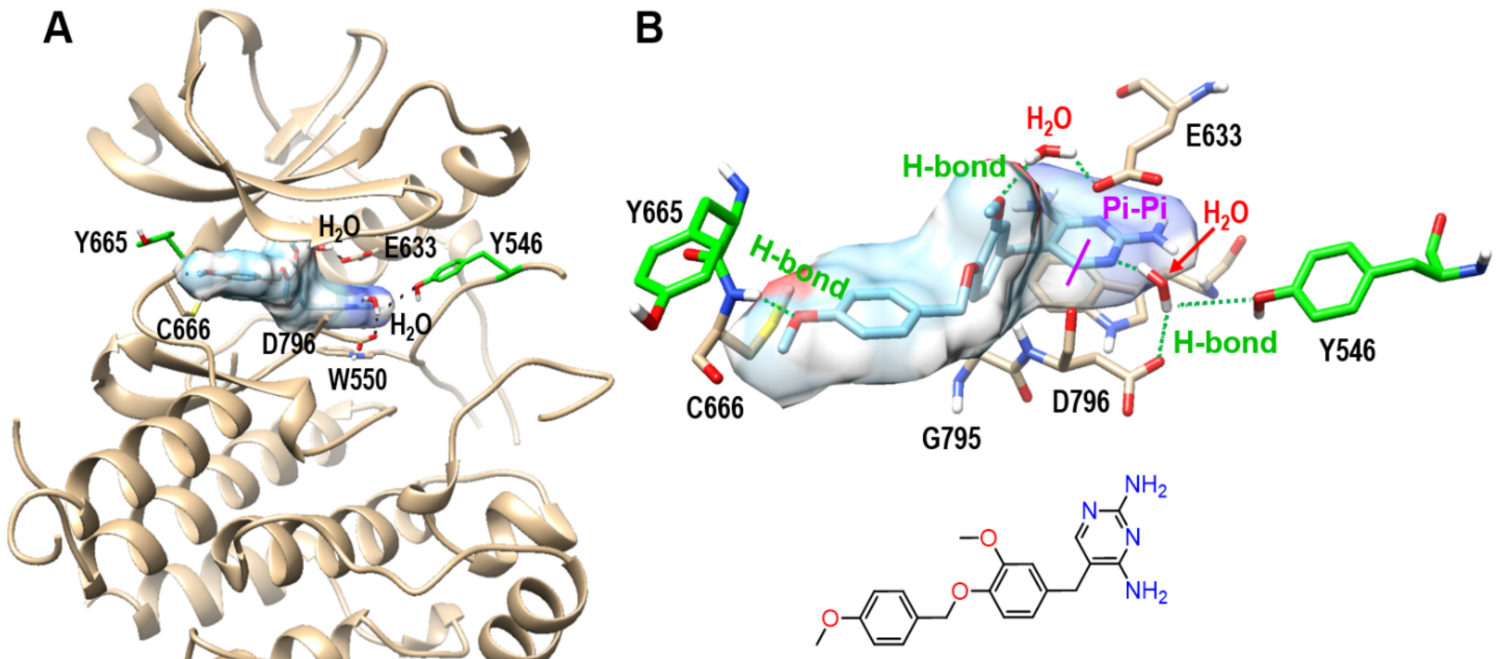

A
Y665
H2O
E633
Y546
C666
D796
H2O
W550
B
H2O
E633
H-bond
Y665
Pi-Pi
H2O
H-bond
H-bond
Y546
C666
G795
D796
NH2
N
N
NH2
O
O
O

Figure S5

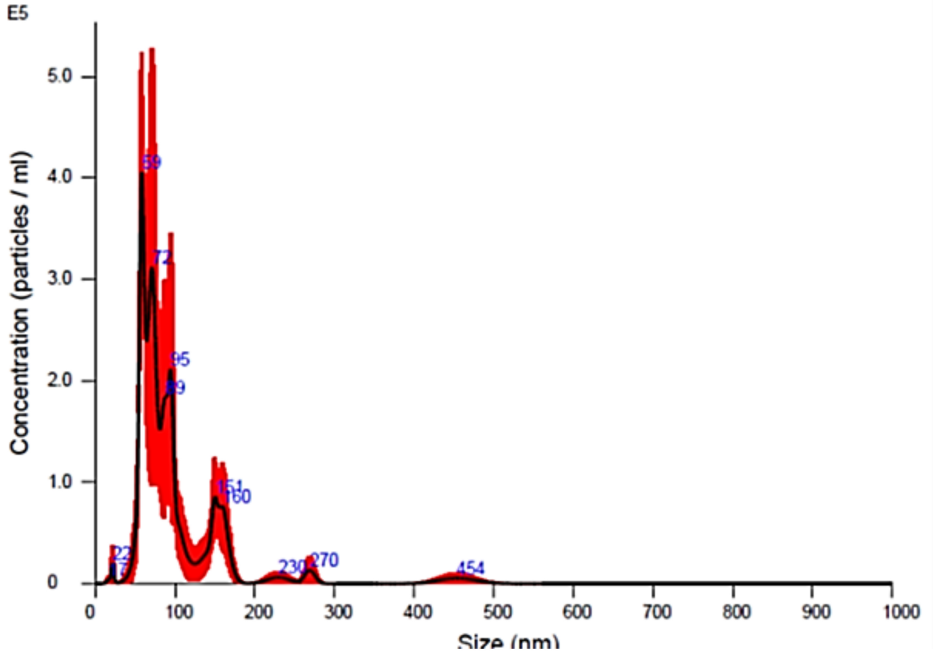
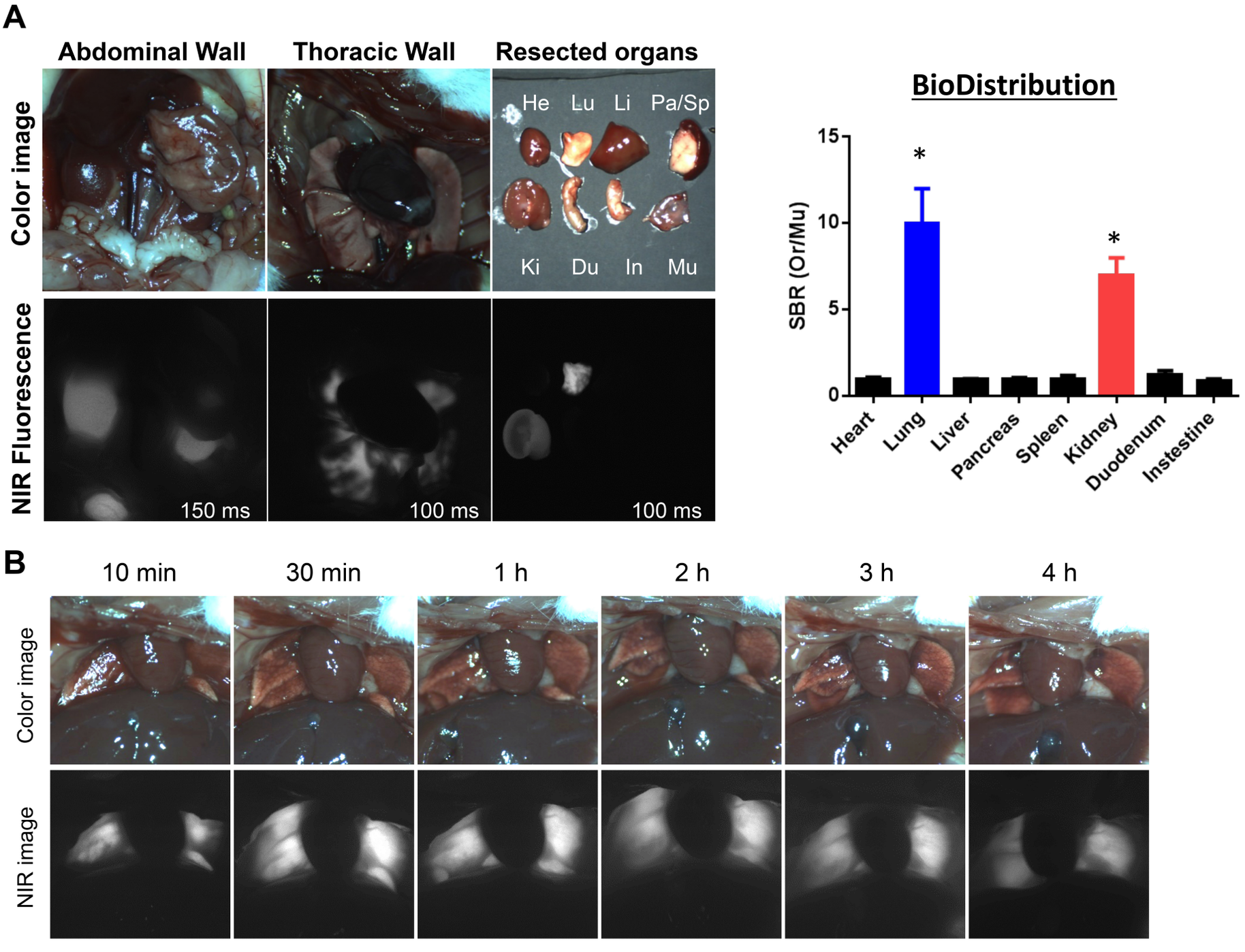
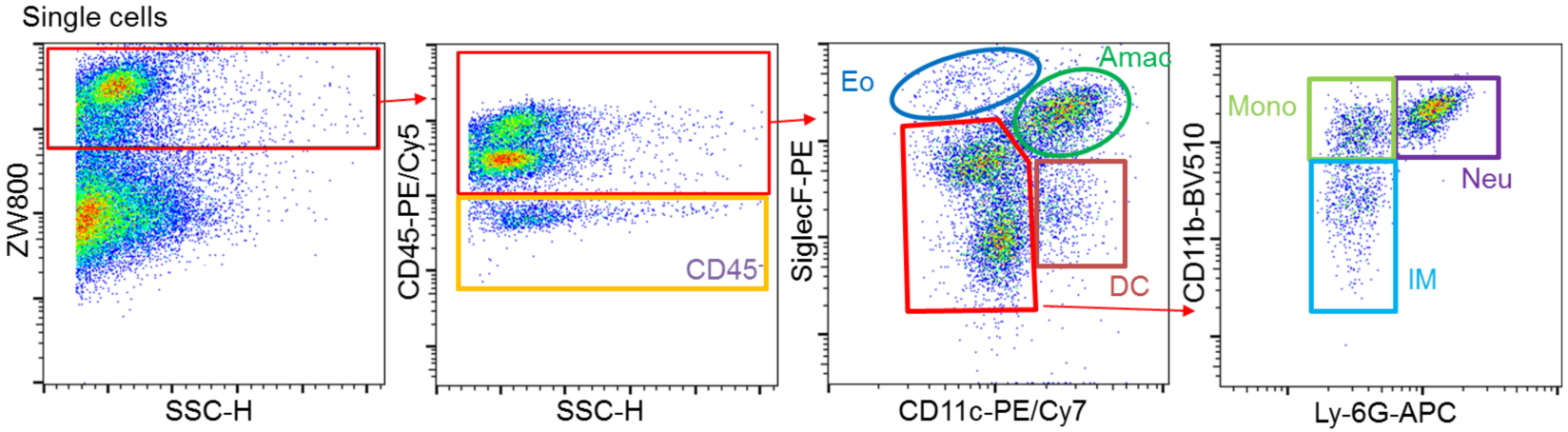

E5
Concentration (particles / ml)
5.0
4.0
3.0
2.0
1.0
0
0
100
200
300
400
500
600
700
800
900
1000
Size (nm)
89
72
95
89
151
160
270
454

Figure S4



Pharmacokinetics	Value
k_{el}	0.004668
Half-life, T1/2β (min)	148.46
AUC (%ID/g·min)	1122
Plasma clearance (mL/min)	0.1783
Volume of distribution (mL)	38.1862

Figure S6


Single cells
ZW800
SSC-H
CD45-PE/Cy5
SSC-H
CD45-
SiglecF-PE
CD11c-PE/Cy7
Eo
Amac
DC
CD11b-BV510
Ly-6G-APC
Mono
Neu
IM

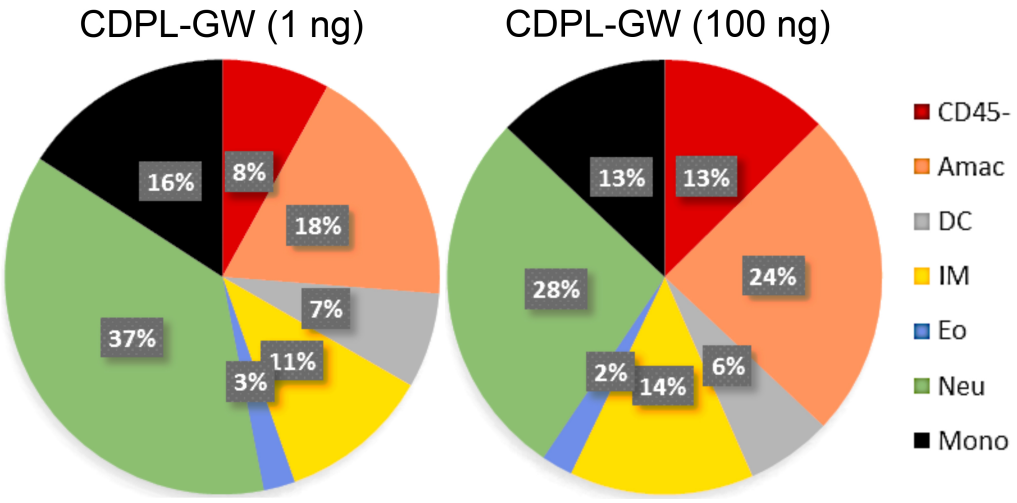

CDPL-GW (1 ng)
16%
8%
18%
7%
37%
11%
3%
CDPL-GW (100 ng)
13%
13%
24%
28%
6%
2%
14%
CD45-
Amac
DC
IM
Eo
Neu
Mono

Figure S7

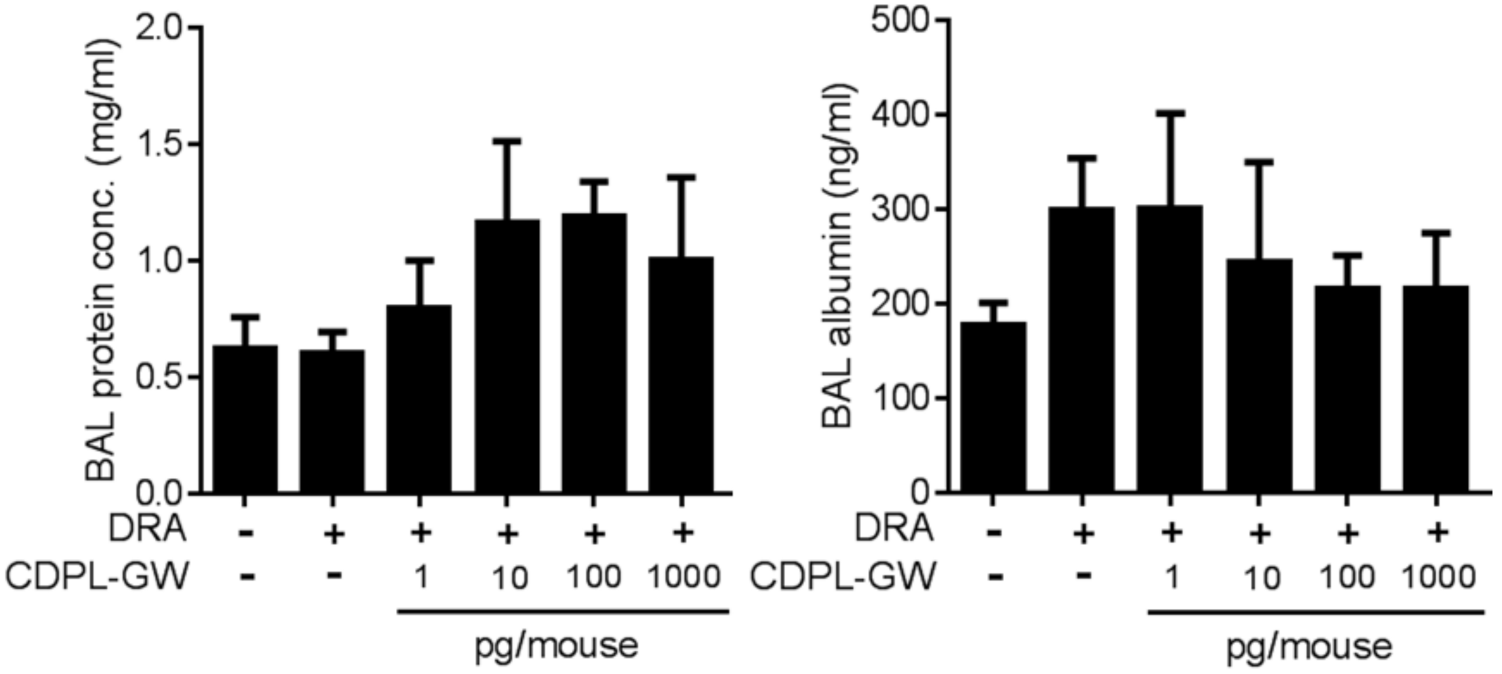
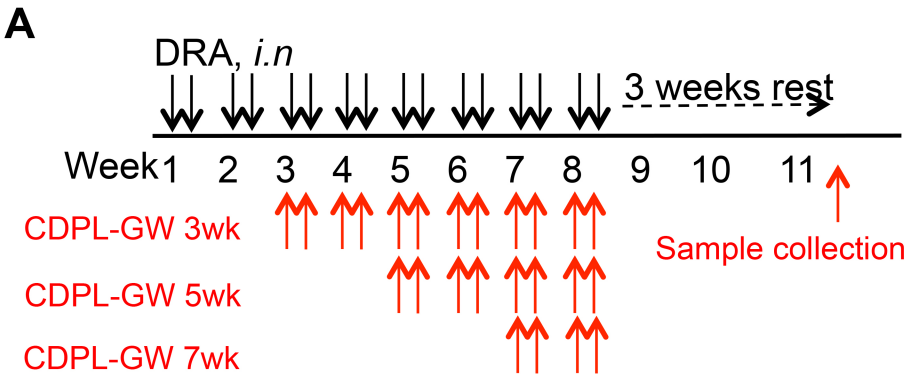
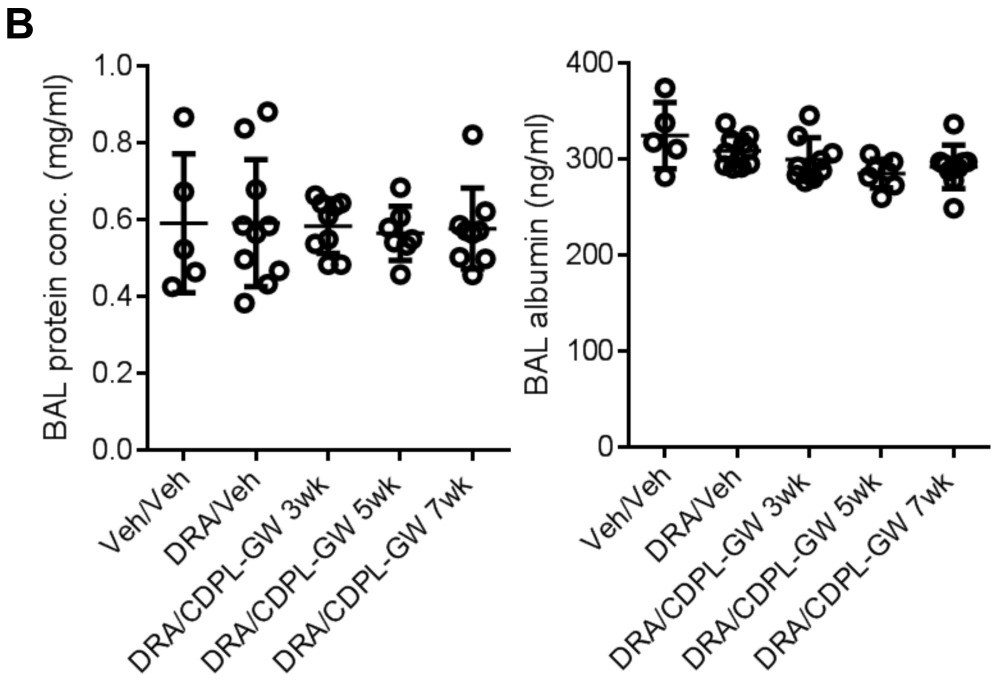

BAL protein conc. (mg/ml)
2.0
1.5
1.0
0.5
0.0
DRA - + + + + +
CDPL-GW - - 1 10 100 1000
pg/mouse
BAL albumin (ng/ml)
500
400
300
200
100
0
DRA - + + + + +
CDPL-GW - - 1 10 100 1000
pg/mouse

Figure S8


A
DRA, i.n
3 weeks rest
Week 1 2 3 4 5 6 7 8 9 10 11
CDPL-GW 3wk
CDPL-GW 5wk
CDPL-GW 7wk
Sample collection


B
BAL protein conc. (mg/ml)
1.0
0.8
0.6
0.4
0.2
0.0
BAL albumin (ng/ml)
400
300
200
100
0
Veh/Veh
DRA/Veh
DRA/CDPL-GW 3wk
DRA/CDPL-GW 5wk
DRA/CDPL-GW 7wk

Supplementary Methods and Figure Legends

ELISA

Mouse CSF1 ELISA kit was purchased from R&D systems (Minneapolis, MN), mouse IL-4, IL-13, IL-17A, and IFN-γ ELISA kits were obtained from eBioscience (Waltham, MA) and anti-mouse IgE ELISA kit was from BioLegend (San Diego, CA). All procedures were followed by the manufacturer's instruction. For measuring DRA-reactive IgE, high affinity-binding 96-well plates were coated with DRA (D.f;100, ragweed;1000 and *Aspergillus*;100 μg/ml, purchased from Greer Lab), in coating buffer for overnight at 4℃. Next, 1% bovine serum albumin (BSA) was used as blocking buffer for 1h at room temperature and the rest of the procedure followed the IgE ELISA kit protocol as we described previously [1].

Flow cytometry

BAL cells, lung tissues, whole blood, and bone marrow were prepared for flow cytometry as described [2]. The lineage markers (Lin) containing anti-mouse CD3 (APC; BioLegend), anti-mouse B220 (APC; BioLegend), anti-mouse TER-119 (APC; BioLegend), anti-mouse F4/80 (APC; BioLegend) and anti-mouse CD64 (APC; BioLegend) were used to exclude T and B lymphocytes, erythrocytes and macrophages from the analysis. Anti-mouse CD11c (PE/Cy7; BioLegend), anti-mouse I-A/I-E (BV605; BioLegend), anti-mouse CD24 (BV510; BioLegend) and anti-mouse CD172a (AF700; BioLegend) used for cDC1 and cDC2 markers. Anti-GFP (AF488; BioLegend) and anti-mouse CSF1R (Percp; R&D systems) used for analyzing CSF1R expression in MAFIA mice. To identify the apoptosis, Annexin V apoptosis detection kit (BioLegend) was used by following the manufacturer's instruction. The analyses for conventional DC populations and CSF1R expression were done by using Kaluza software (Beckman Coulter, Indianapolis, IN).

Histology, Immunohistochemistry(IHC) & Periodic acid Schiff (PAS) staining

Formalin-fixed and paraffin-embedded sections of lung tissues were used for H&E, Immunohistochemistry (IHC), and Periodic acid-Schiff (PAS) staining. The primary antibodies used for the studies include anti-CSF1, anti-collagen, and anti-αSMA antibodies (Abcam, Cambridge, MA). Histologic tissue processing and analyses were performed by Research Histology and Tissue Image Core (RHTIC) at UIC. All of the images were photographed using an Olympus BX51 fluorescence microscope (Olympus).

Measurement of Bronchial hyper-responsiveness

Mice were anesthetized with ketamine/xylazine mixture, and a tracheostomy tube was inserted. Mechanical ventilation was initiated using a Flexivent small animal ventilator (Sireq, Montreal, QC). Continuous EKG and pulse oximeter monitoring was performed. Airway resistance was measured after sequentially increasing doses of methacholine as described previously [3].

Synthesis of β-cyclodextrin (β-CD) conjugated epsilon-polylysine (CDPL)

CDPL was prepared by our previous developed method [4]. Briefly, to oxidize a hydroxyl group of β-cyclodextrin (β-CD), β-CD (1 g) and Dess–Martin periodinane (0.8 g) were dissolved in anhydrous DMSO (25 mL) and stirred for 12 h at room temperature. The reaction mixture was washed with cold acetone several times by precipitation method to remove insoluble impurities and the white solid dried in vacuum. An aldehyde-CD (700 mg) was dissolved in 25 mL of acetate buffer (0.2 M, pH 4.5) and then mixed with epsilon-polylysine (100 mg). After stirring for 1 h, sodium triacetoxyborohydride (263 mg) was added into the reaction mixture, followed by stirring for additional 72 h. Dialysis was carried out in cellulose membrane with a molecular weight cutoff (MWCO) of 12-14 kDa for 24 h against deionized water, and the resulting solution was freeze-dried. To visualize the CDPL nanoparticle, NIR fluorophore (ZW800-1C) was conjugated onto the CDPL chain using the conventional N-Hydroxysuccinimide (NHS) ester chemistry. Finally, succinic anhydride (half amount of the number of amines on CDPL chain) added into ZW800-CDPL in PBS (pH 8.0) to convert the surface charge from positive to zwitterionic and the resulting mixture was washed with acetone and dried in vacuum.

Preparation of GW2580-CDPL Inclusion complex

CDPL (2.5 μM in water) was mixed with GW2580 solution (20 μM in DMSO/PBS, 50/50 v/v%) and the mixture was vortexed for 24 h at room temperature. Then, the unbound GW2580 was removed by using micro Bio-Spin P-6 gel columns (Bio-rad). The absorbance of purified CDPL-GW solutions was then measured at around 280 nm to calculate the amount of GW2580.

***In vivo* bio-distribution and pharmacokinetics of GW2580-CDPL**

Animals were housed in an AAALAC-certified facility and were studied under the supervision of Massachusetts General Hospital (MGH) Institutional Animal Care and Use Committee (IACUC) in accordance with the approved institutional protocol (#2016N000136). Six weeks old CD-1 mice (male; 25-30 g) were purchased from Charles River Laboratories (Wilmington, MA). Mice were maintained under anesthesia by inhalation of

isoflurane or intraperitoneally injection with 100 mg/kg ketamine and 10 mg/kg xylazine (Webster Veterinary, Fort Devens, MA). The end of the tail was cut to be enable blood extraction. Before injection, blood was then sampled in heparinized capillary tubes (Fisher Scientific, Pittsburgh, PA) as a reference and collected blood was stored in an ice box to prevent clotting. Mice were injected with 10 nmol of CDPL-GW in saline and blood was collected to estimate blood half-life. Mice were imaged using the in-house built real-time intraoperative NIR imaging system. A 760 nm excitation laser source (4 mW/cm) was used with white light (400–650 nm; 40,000 lux). After 4 h post-injection, mice were sacrificed to evaluate the biodistribution of CDPL-GW in organs.

Molecular Docking Study of CSF1R kinase domain

The crystal structure of CSF1R Kinase was downloaded from the RCSB protein data bank and prepared by the Protein Preparation Wizard in Schrödinger 2016 [5]. During the protein preparation procedure, hydrogens were added and partial charges were assigned in the OPLS3 force field [6], and then all the added hydrogens were minimized. The 3D structure of the GW2580 was processed by LigPrep module of Schrödinger2016 [7] and then the GW2580 was docked into the above prepared CSF1R Kinase using GOLD v5.2.2 [8]. GW2580 was set to be flexible, while the CSF1R Kinase was set to be rigid. Standard default settings were used for other parameters. The binding poses for GW2580 were evaluated using the ChemPLP scoring function [9] and the top scoring docking conformation was selected.

References

1. Moon H-G, Kim S-j, Jeong JJ, et al. Airway Epithelial Cell-Derived Colony Stimulating Factor-1 Promotes Allergen Sensitization. *Immunity.* 2018;49(2):275-287.e275.
2. Moon HG, Tae YM, Kim YS, et al. Conversion of Th17-type into Th2-type inflammation by acetyl salicylic acid via the adenosine and uric acid pathway in the lung. *Allergy.* 2010;65(9):1093-1103.
3. Grozdanovic M, Laffey KG, Abdelkarim H, et al. Novel peptide nanoparticle-biased antagonist of CCR3 blocks eosinophil recruitment and airway hyperresponsiveness. *J Allergy Clin Immunol.* 2018.
4. Kang H, Gravier J, Bao K, et al. Renal Clearable Organic Nanocarriers for Bioimaging and Drug Delivery. *Adv Mater.* 2016;28(37):8162-8168.
5. Schrödinger Release 2016-1: Schrödinger Suite 2016-1 Protein Preparation Wizard; Epik version 3.5, Schrödinger, LLC, New York, NY; Impact version 7.0, Schrödinger, LLC, New York, NY; Prime version 4.3, Schrödinger, LLC, New York, NY. 2016.
6. Jorgensen WL, Maxwell DS, TiradoRives J. Development and testing of the OPLS all-atom force field on conformational energetics and properties of organic liquids. *J Am Chem Soc.* 1996;118(45):11225-11236.
7. Schrödinger Release 2016-1: ligprep, version 3.7, Schrödinger, LLC, New York, NY. 2016.
8. Verdonk ML, Cole JC, Hartshorn MJ, Murray CW, Taylor RD. Improved protein–ligand docking using GOLD. *Proteins: Structure, Function, and Bioinformatics.* 2003;52(4):609-623.
9. Korb O, Stützle T, Exner TE. Empirical Scoring Functions for Advanced Protein−Ligand Docking with PLANTS. *Journal of Chemical Information and Modeling.* 2009;49(1):84-96.

Figure Legends for Online Supplemental Figures.

Supplementary figure 1. (A) FACS strategy to identify alveolar cDC1 and cDC2 in BAL fluids. Lineage markers were defined in Methods. **(B)** In steady state, $CSF1R^+$ cDCs were highly populated in the respiratory system, whereas the numbers of $CSF1R^+$ cDCs were very low in bone marrow and blood. Of note, $CSF1R^+$ cDC2s only emerged in BAL fluid, although $CSF1R^+$ cDC1 resided highly both in the lung and BAL fluid.

Supplementary figure 2. (A) All of the mice were challenged with DRA as depicted in the experimental scheme. For the depletion of the AEC-derived CSF1, Tm (75mg/kg) was given by oral gavage to *Scgb1a1-cre*ERT;*Csf1*$^{fl/fl}$ ($CSF1^{\Delta AEC}$) mice. CSF1 (brown) is highly expressed in airway epithelial cells in DRA-challenged, but not sham-treated mice (Vehicle only). Administration of Tm depleted CSF1 expression, which was restored at 6 weeks after Tm administration. The contralateral lung was used for measuring CSF1 by ELISA. Tm treatment resulted in an immediate reduction in lung CSF1, which was restored to baseline by week 4. The scale bars represent 200 μm. * $p<0.05$.

Supplementary figure 3. Binding pose of the compound GW2580 with CSF1R from co-crystal complex. (A) Binding pose of GW2580 in CSF1R kinase domain. (B) Interactions of pivotal residues of CSF1R kinase domain with compound GW2580. The residues of CSF1R kinase domain are colored in tan, while GW2580 is colored in cyan. Hydrogen bond interactions are in black dash lines. H-Bonds were found for GW2580 with backbones of E664, C666, D796 and sidechain of T663. And W550 and Y665 form π- π stacking interactions with phenyl and heterocycle rings of GW2580, respectively. Hydrophobic interactions are detected for A614, V647, L769, F797 and GW2580.

Supplementary figure 4. Biodistribution and pharmacokinetics of CDPL-GW nanoprobes in mice. 60 nmol of CDPL-GW in saline was delivered intranasally into lungs and signals were measured in multiple organ (A-B), and SBR of lung tissues (C), blood half-life (D), and pharmacokinetic parameters (E) were observed over the time course of 4 h post-administration (n = 3, mean ± s.d.). kel, elimination rate constant; t1/2,β, elimination half-life; AUC, area under the curve. *$p<0.05$

Supplementary figure 5. The size distribution of CDPL-GW nanoparticles as measured by NanoSight.

Supplementary figure 6. Cellular distribution of CDPL-ZW by intranasal delivery. By tracing the fluorophore ZW800-1 of CDPL-GW, we evaluated the distribution of CDPL-GW by counting the fluorescent cells by flow

cytometry. Each 1 ng and 100 ng of CDPL-GW per mouse was delivered via the intranasal route. In 2 hours, lung tissues were made into single cell suspensions. Single cell suspensions from the lung were gated into the positive ZW800, after which the cells were identified by cell specific markers.

Supplementary figure 7. Mice were subject to the experiment scheme depicted in Figure 5B. The concentrations of BAL protein and albumin were measured as the increasing doses of CDPL-GW were delivered via the intranasal route.

Supplementary figure 8. (A) Experimental scheme for figure 6. CDPL-GW treated in three different time points, from 3 to 8 weeks, from 5 to 8 weeks and from 7 to 8 weeks. (B) The concentrations of BAL protein and albumin were measured after 3 weeks of resting since last DRA challenge.